



Working Report 2007-29

Far-Field Thermal-Mechanical Response of One- and Two-Storey Repositories in Olkiluoto

Kari Ikonen

May 2007

Working Report 2007-29

Far-Field Thermal-Mechanical Response of One- and Two-Storey Repositories in Olkiluoto

Kari Ikonen

Technical Research Centre of Finland
(VTT)

May 2007

Working Reports contain information on work in progress
or pending completion.

The conclusions and viewpoints presented in the report
are those of author(s) and do not necessarily
coincide with those of Posiva.

FAR-FIELD THERMAL-MECHANICAL RESPONSE OF ONE- AND TWO-STOREY REPOSITORIES IN OLKILUOTO

ABSTRACT

This report contains results from far-field temperature and deformation analysis of the spent nuclear fuel repository in Olkiluoto. The objective of the analyses was to determine dimensions of the tensile stressed bedrock above the repository near the ground surface. Tensile stresses may open fractures in rock mass and ground water flow may become faster, if suitable pressure differences exist and further, potential for radionuclide transport from leaking canisters becomes higher to upward direction, towards biosphere. In considering stress state far from the rectangular repository the most essential parameters are the length, width and depth of the repository and the total decay heat density. Other details, like vertical or horizontal orientation of canisters is of less importance when considering situation far from the repository. The absolute value of the stress locally in the bedrock depends remarkably on the existing compressive natural in-situ stresses, which have different values in various orientations. The estimated Olkiluoto in-situ stresses based on the site characterization investigations have been taken into account.

The depth in tensioned volume extends in the one-storey repository to the depth of 94...107 m after about 300 years and in the two-storey repository to the depth of 129...146 m. The maximum tensile strain on the ground surface is about 0.00024 after about 600 years. Two-dimensional plane strain analyses gave conservative results when compared with more realistic three-dimensional analyses. When assuming the decreased deformation modulus for the rock mass due to the tensile cracking very conservatively the maximum depth of the tensile stressed rock is increased at most 10%. Ground uplift reaches its maximum of 6.9 cm about 1 230 years in the one-storey repository and 12.6 cm in the two-storey repository after about 1 400 years.

Keywords: TM analyses, far-field stresses in repository for spent nuclear fuel, repository, Olkiluoto, decay heat

KAUKOKENTÄN TERMOMEKAANINEN VERTAILU OLKILUODON LOPPUSIJOITUSTILAN YKSI- JA KAKSIKERROSRATKAISUISSA

TIIVISTELMÄ

Raportissa kuvataan Olkiluodon käytetyn ydinpolttoaineen loppusijoitustilan kallioon synnyttämien lämpötila- ja muodonmuutoskenttien laskentatulokset. Analyysillä pyrittiin määrittämään vetojännitettyjen kallioilavuuksien dimensiot sijoitustilan yläpuolella maanpinnan läheisyydessä. Vetojännitetyillä alueilla kallion luontaiset säröt saattavat avautua, pohjavesivirtaukset saattavat lisääntyä ja kapseleista mahdollisesti vuotavien radionuklien kulkeutuminen ylöspäin helpottua. Tarkasteltaessa jännitystilaa kaukana loppusijoitustilasta sen ominaisuuksista merkittävimmin vaikuttavat suorakaiteen muotoisen sijoitustilan pituus, leveys ja syvyys sekä kapseleiden lämpöteho pinta-alaa kohti. Yksityiskohdilla kuten kapseleiden sijoituksella pysty- tai vaakasentoon ei ole merkitystä tarkasteltaessa tilannetta kaukana kapseleista. Vetojännityksen todelliseen suuruuteen alentavasti vaikuttaa kallion luonnollinen (in-situ) paikallinen puristusjännitys, joka vaihtelee eri suunnissa. Laskelmissa on huomioitu Olkiluodon kalliooperän mittauksista arvioidut kallion erisuuntaiset in-situ-jännityskomponentit.

Vetojännitetyn kallioilavuuden maksimisyvyys yksikerrosratkaisussa on 94...107 m noin 300 vuoden kohdalla ja kaksikerrosratkaisussa 129...146 m. Maksimivenymä maan pinnalla on noin 0,00024 noin 600 vuoden kohdalla. Laskelmat antoivat tulokseksi, että tasovenymämalli antaa konservatiivisia tuloksia realistisempaan kolmeulotteiseen malliin verrattuna. Kallion halkeilun hyvin konservatiivinen huomioonottaminen lisää vetojännitetyn kallioilavuuden maksimisyvyyttä enintään 10 %. Maanpinnan kohoaminen saavuttaa maksiminsa 6,9 cm noin 1 230 vuoden kuluttua yksikerrosratkaisussa ja 12,6 cm kaksikerrosratkaisussa noin 1 400 vuoden kuluttua.

Avainsanat: TM-analyysi, loppusijoitustilan globaalit lämpöjännitykset, loppusijoitustila, Olkiluoto, jälkilämpö

TABLE OF CONTENTS

ABSTRACT

TIIVISTELMÄ

1	INTRODUCTION	3
2	INITIAL DATA	6
	2.1 Geometry and dimensions of calculation model	6
	2.2 Thermal-mechanical properties of materials	8
	2.3 Exponential decay heat modelling	10
3	CALCULATION METHOD	12
	3.1 Analytical solution of rock temperatures	12
	3.2 Modelling of rock mechanics conditions.....	13
	3.3 Principal stresses	14
	3.4 Modelling of fractured rock on tensile stressed volumes	16
	3.5 Analyzing procedure	16
4	TWO-DIMENSIONAL ANALYSES	17
	4.1 One-storey repository with intact rock mass model	17
	4.2 Two-storey repository with tension fractured rock mass model	21
	4.3 Effect of depositing rate	23
	4.4 Conclusion from 2D analysis.....	23
5	THREE-DIMENSIONAL ANALYSES	24
	5.1 Conclusion from 3D analysis.....	30
6	CONCLUDING REMARKS.....	32
	ACKNOWLEDGEMENT	34
	REFERENCES	35

LIST OF SYMBOLS

LATIN ALPHABET

A	surface area
c	heat capacity
d	thermal diffusivity
E	deformation modulus
g	gravitational acceleration (= 9.81 m/s ²)
H	height of vertical line heat source
H_{eff}	effective height of vertical line heat source
P	power
r_0	canister radius
T	temperature
t	time
V	volume
x, y, z	cartesian co-ordinates

GREEK ALPHABET

λ	heat conductivity
ρ	density
ν	Poisson's ratio
σ	stress
σ_H	maximum horizontal initial stress in rock
σ_h	minimum horizontal initial stress in rock
σ_{maj}	major principal stress
σ_v	vertical initial stress in rock
τ	shear stress

SPECIAL NOTATIONS

EPR	European pressurized water reactor
2D	two-dimensional
3D	three-dimensional
TM	thermal-mechanical

1 INTRODUCTION

According to the Finnish programme for spent fuel management a repository is planned to be constructed in the deep bedrock in Olkiluoto. Figure 1 shows the principal layout of the repository. In the base design case the repository is in the dept of 400 m. Each panel has a central tunnel area, whose width is 86 m measured from the closest canister centres on opposite side of the central tunnel. In one panel, the maximum length of a deposition tunnel is 350 m.

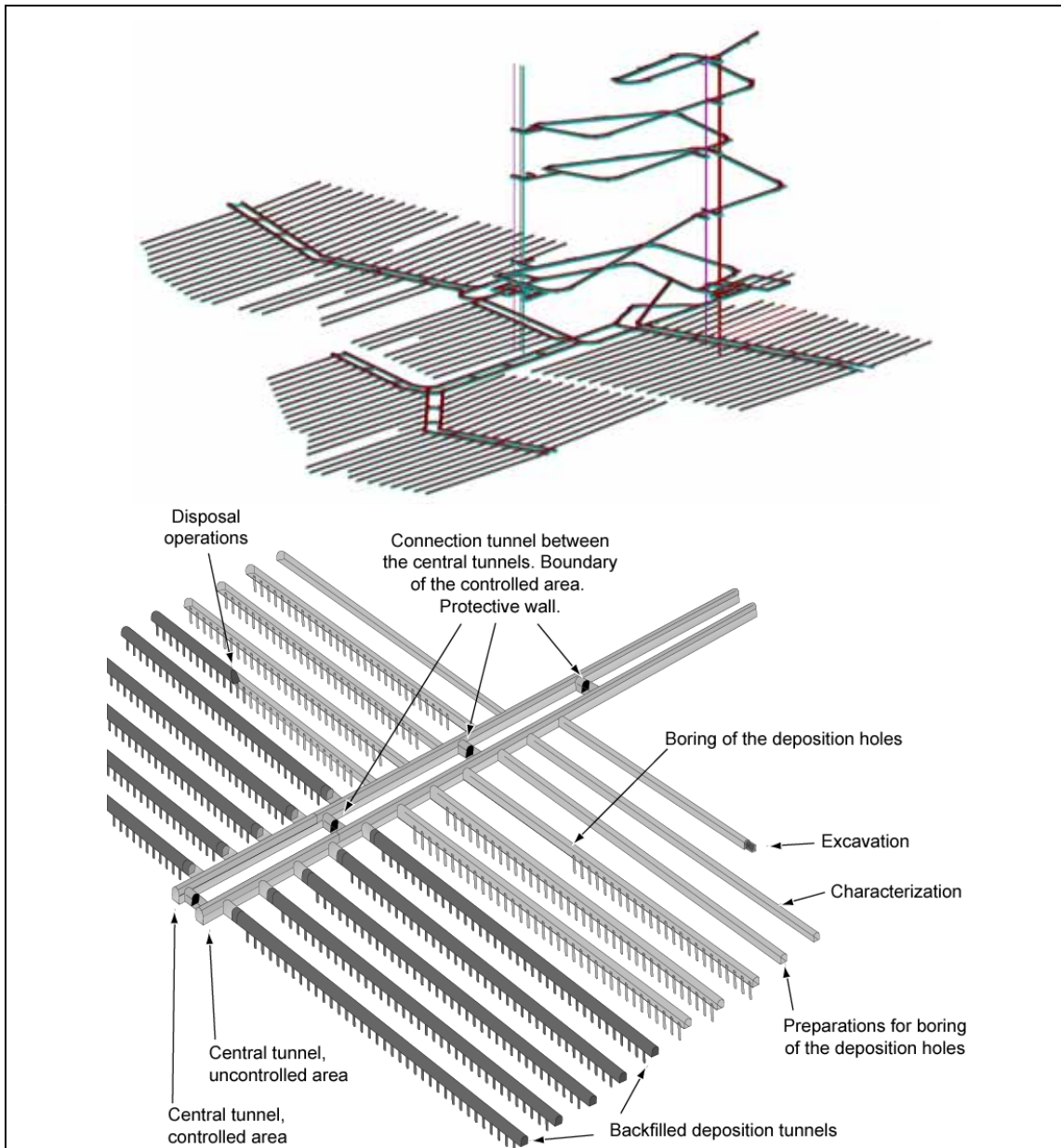


Figure 1. Principal layout of the repository (Posiva Oy).

The target of this work is to give an estimate of the depth and volume of the amount of bedrock above the repository that becomes in a tension stress condition due to thermal deformation in the long-term evolution. The numerical model used to this simulation is an engineering approach and it can not be used to predict the initiation of rock cracking or the crack growth of the existing cracks but to predict the size and volume of the bedrock that becomes in tension stress condition from the natural compression state. In addition, the time dependency of the stress state changes can be estimated.

The result is used in repository safety case to assess the possible changes in ground water flow conditions (water conductivity or transmissivity) due to loosening or opening of the existing crack system or crushed zones that are the main flow network of the ground water in bedrock. To practically estimate the general water flow pathway opening tendency of the existing crack network, the first assessment parameter is the principal strain, not the principal stress.

A lot of numerical sensitivity studies were made in 2D prior the essential numerical 3D model could be reliably made. For example the overall dimension of the model, the boundary conditions, the mesh density of the finite elements, and the essential time window of the thermal effects were investigated and defined with the simpler 2D-model that is possible to run in the computer in a few minutes as the heavier 3D runs require a few hours each run even in the very fast computing workstations available at VTT (the Technical Research Centre of Finland). Only a few of the sensitivity studies, as an example, with 2D model are included in the report. Actually, the 2D results differ only a little from the 3D results and they are on the conservative side.

In calculation model, totally there are 932 EPR-canisters in one panel. It takes 45 years to deposit all the canisters to one panel, when the depositing rate is 20.7 canisters per year. The canister spacing 10 m was chosen according to the earlier analyses and the spacing of the tunnels was set to 25 m.

In considering situation at large distance from the repository the most essential parameters are the length, width and depth of the repository and the total decay heat power. Other details, like vertical or horizontal orientation of canisters, or orientation of deposition tunnels, is of less importance when considering situation far from the repository.

In this study local stresses near canisters and tunnels are not investigated. Thus canister and tunnel volumes are not modelled in detail, but these areas are assumed to be solid and they are modelled by fairly coarse finite element mesh. Stresses near canisters and tunnels are studied for instance in (Olkiluoto Site Description 2004) and (Jussila 1997).

The temperature fields in the bedrock were determined by superposing analytic line heat source models (Ikonen 2003, Ikonen 2005). Thermal-mechanical finite element 2D and 3D analyses were performed with the *PASULA* computing package, which has been developed at VTT for a variety of structural analysis and heat conduction capabilities.

As will be shown later, the actual planned deposition rate and the simultaneous deposition (all canisters are deposited at a time) give practically equal maximum long-time

far-field quantities like tensile stressed depth of the rock or the uplift of the ground surface. This is useful observation in reducing 3D finite element model.

Earlier analyses (Ikonen 2003) showed that in case of two-storey repository the decay power of the later deposited lower storey should be lower than the decay power of the first deposited storey due to thermal interaction between the upper and lower storeys. In the analyses performed in this study the upper and lower storeys are conservatively assumed to be identical and have equal thermal power.

2 INITIAL DATA

In the following, dimensions and layout of the calculation model, thermal-mechanical properties of materials and decay heat expression are presented.

In the depth of 400 m the ambient rock temperature in Olkiluoto is $+10.5^{\circ}\text{C}$ and the ambient temperature increases $+1.5^{\circ}\text{C}$ per 100 meters in depth direction. This initial temperature is now not applied, since only changes, concerning stresses and deformations, from the initial state are considered.

2.1 Geometry and dimensions of calculation model

Figure 2 shows the dimensions and layout of the calculation model. The width 4 000 m and the height 2 000 m of the model were determined by trial-and-error method so far from the repository that the disturbances from the repository area do not reach the right and left vertical and horizontal lower planes. The displacements were constrained in the nodes lying on the end planes.

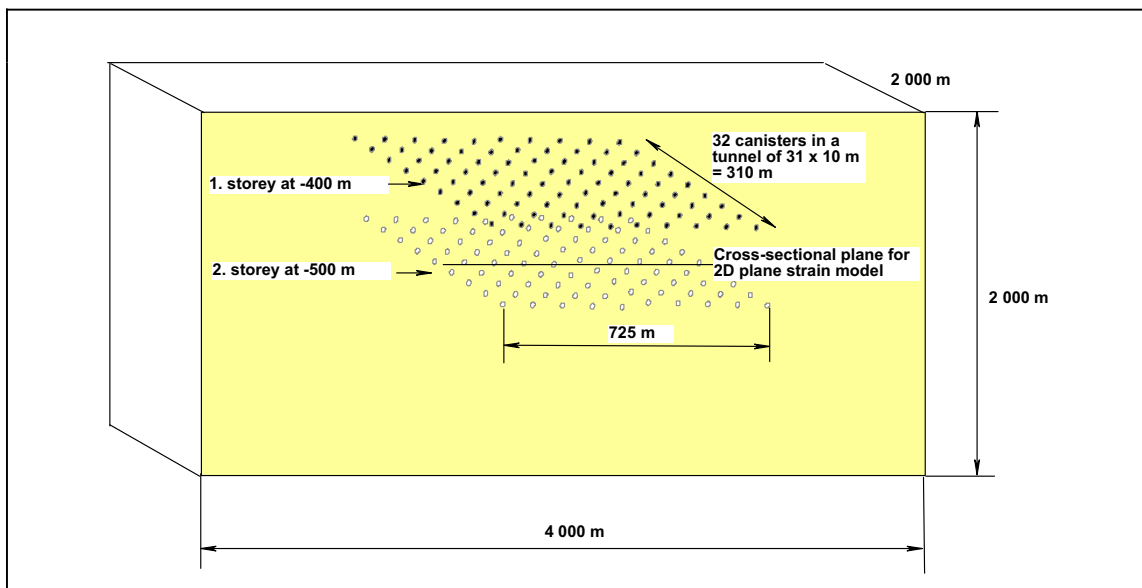


Figure 2. Dimensions of calculation model area.

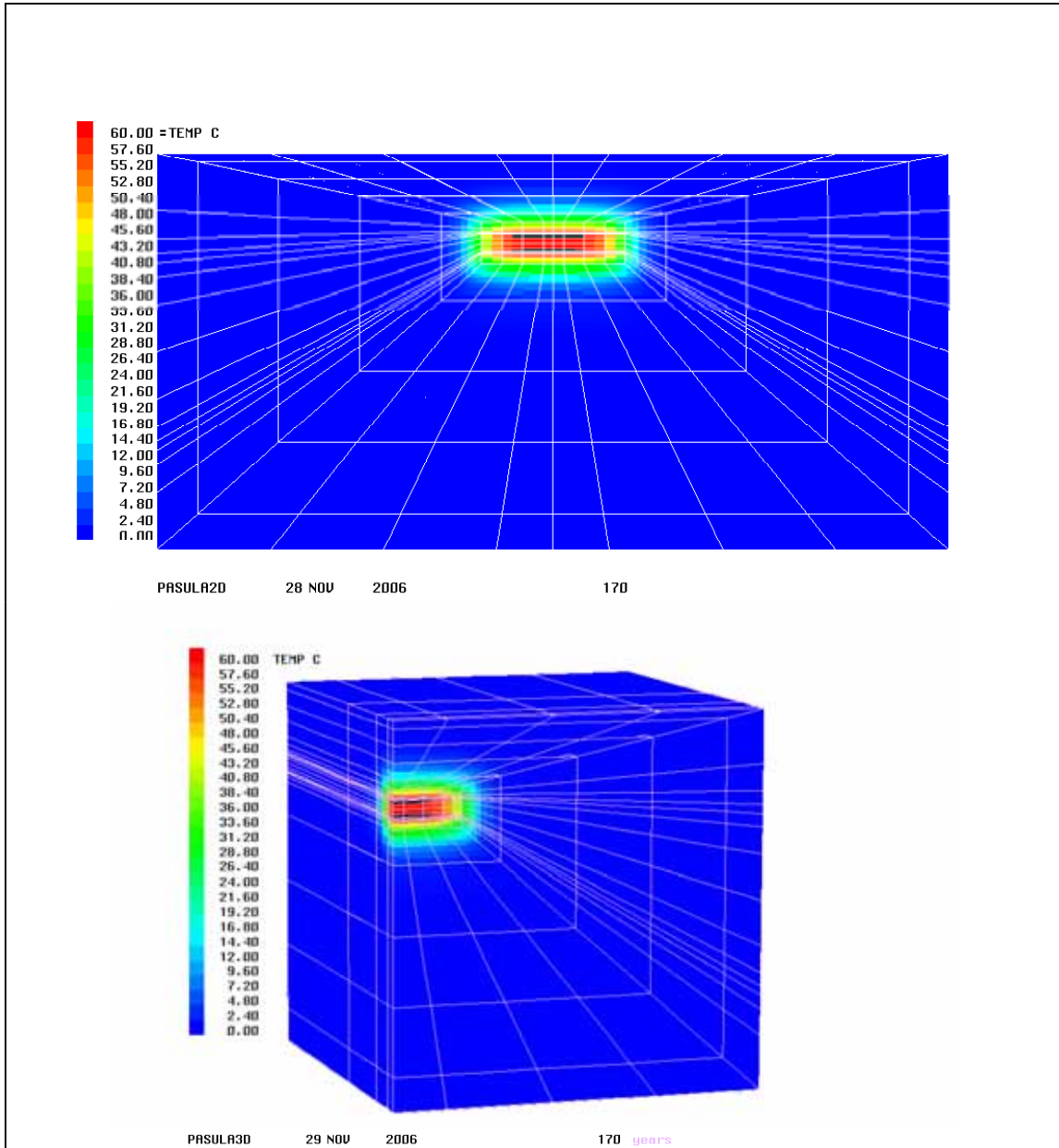


Figure 3. Examples of 2D and 3D finite element meshes showing also temperatures and deformations.

Figure 3 shows examples of 2D and 3D finite element meshes.

2.2 Thermal-mechanical properties of materials

The conductivity of Olkiluoto rock and heat capacity are based on laboratory measurements with core drilled samples (Kukkonen 2000). The conductivity of the rock decreases slightly as a function of temperature and at temperatures of 22°C, 60°C and 100°C the conductivity is 2.70 ± 0.42 , 2.61 and 2.49 W/m/K, respectively (Figure 4). The constant average value of 2.61 W/m/K (at 60°C) consistent with earlier analysis (Ikonen 2003) and (Ikonen 2005) for the Olkiluoto repository is used in this study.

The heat capacity of the rock increases slightly as a function of temperature and at the temperatures of 22°C, 60°C and 100°C the capacity is 737, 784 and 832 ± 19 J/kg/K, respectively (Figure 4). The value of 784 J/kg/K (at 60°C) consistent with earlier analysis (Ikonen 2003) and (Ikonen 2005) is used throughout the analysis. With the rock density of 2749 kg/m^3 the applied volumetric heat capacity of the rock material is $2.15\text{ MJ/m}^3/\text{K}$. The diffusivity $1.21\cdot 10^{-6}\text{ m}^2/\text{s}$ (at 60°C) consistent with earlier analysis is used throughout the analysis.

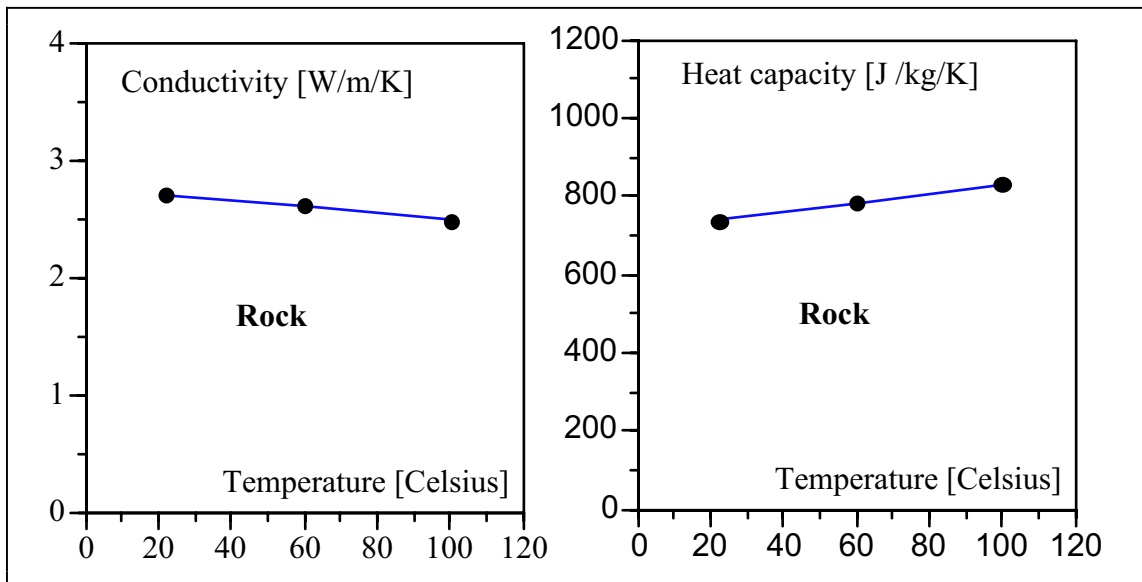


Figure 4. Conductivity and heat capacity of Olkiluoto rock (Kukkonen 2000).

Mechanical properties of the rock mass (in large scale) used in analyses are: deformation modulus 50 GPa generally and 50 or, very conservatively, 25 GPa in-situ fractured rock volumes in tension (Table 5.11 in Posiva 2005). The use of the two upper and lower bound values for the deformation modulus gives an estimate range of the actual behaviour of in-situ fractured rock mass. Poisson's ratio is taken as an average of 0.25. The thermal expansion coefficient is $9.5 \cdot 10^{-6}$ 1/K according to Table 5.7 in Posiva 2005.

According to current operation plan the deposition of 932 canisters in one panel takes 45 years. The deposition rate is then 20.7 canisters per year. The length of a panel is $29 \cdot 25 = 725$ m and the width = $31 \cdot 10$ m = 310 m. The average power density of the panel at the deposition is $1\,830$ W / (25 m \cdot 10 m) = 7.3 W/m². Table 1 summarizes thermal-mechanical properties and other initial data used in the analyses.

Table 1. Initial data used in analyses.

Burn-up value of the spent fuel	50	MWd/kgU
Pre-cooling time of the fuel	49.9	years
Decay heat per canister when deposited	1 830	W
Deposition rate	20.7	canisters per
Canister spacing	10	m
Tunnel spacing	25	m
Canisters in one panel	932	-
Canisters in one tunnel	32	-
Number of tunnels in one panel	30	-
Depth of first panel	-400	m
Depth of the optional second panel	-500	m
Rock conductivity at 60°C	2.61	W/m/K
Rock volumetric heat capacity	2.15	MJ/m ³ /K
Deformation modulus of the rock	50	GPa
Density of rock material	2 749	kg/m ³
Poisson's ratio	0.25	-
Thermal expansion coefficient of the	$9.5 \cdot 10^{-6}$	1/K

Decay heat modelling in described in Chapter 2.3.

2.3 Exponential decay heat modelling

The decay heat decreases strongly with time and, for example, after about 50 years the decay heat is only a half of the amount it was during deposition. The decay power of the spent EPR fuel was calculated by M. Anttila (Anttila 2005) with the ORIGEN-S computer code of the TRITON functional module of the SCALE program package (Oak Ridge National Laboratory 2004). Reasonable decay heat level is reached in 50 years cooling time, if the burn-up value is 50 MWd/kgU. Figure 5 shows decay power of EPR fuel according to ORIGEN-S calculations.

Numerical values of the decay power are shown in Table 2 in the third column. Decay power is presented by a sum of exponential terms

$$P = P_1 \sum_{i=1}^N a_i e^{-\frac{t-t_1}{t_i}}, \quad (1)$$

where P_1 is the power at the first time t_1 , for which 20 years is chosen (after removing the fuel from the reactor). For determining the coefficients a_i the power is satisfied at chosen times giving a system of equations

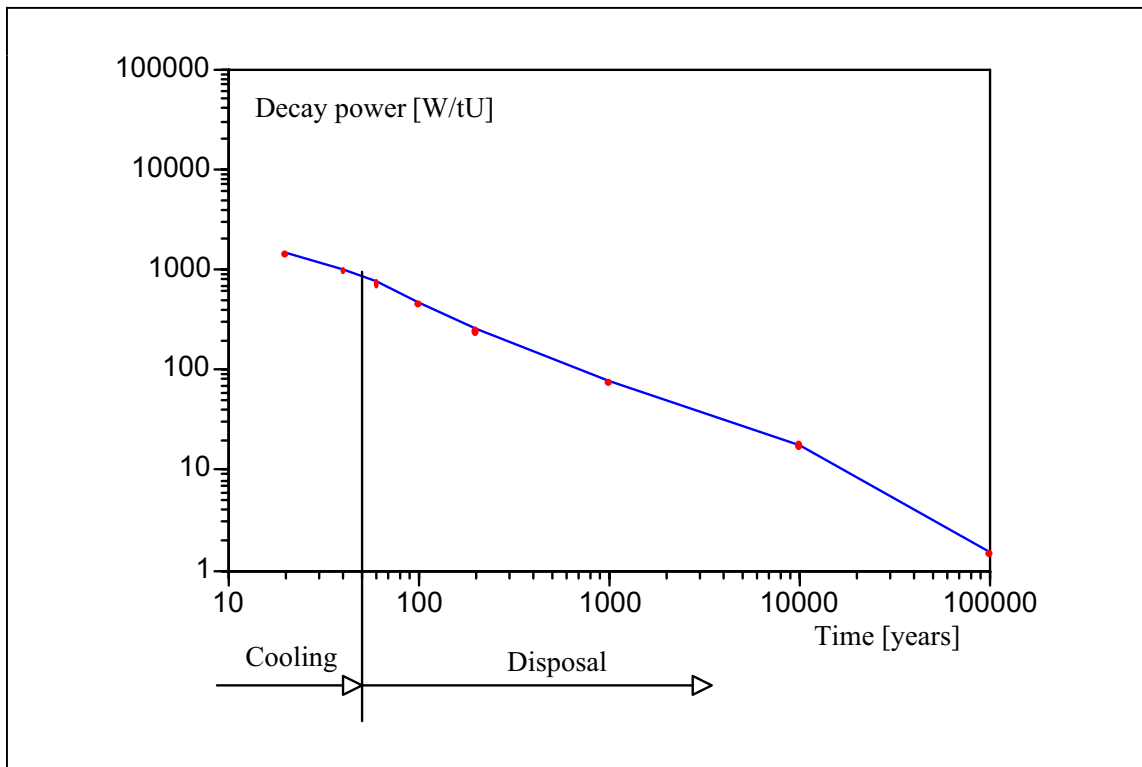


Figure 5. Decay heat of EPR fuel, burn-up 50 MWd/kgU according to (Anttila 2005).

$$\begin{pmatrix} P_1 \\ P_2 \\ P_3 \\ \vdots \end{pmatrix} = P_1 \begin{bmatrix} 1 & 1 & 1 & \dots \\ e^{(t_2-t_1)t_1} & e^{(t_2-t_1)t_2} & e^{(t_2-t_1)t_3} & \dots \\ e^{(t_3-t_1)t_1} & e^{(t_3-t_1)t_2} & e^{(t_3-t_1)t_3} & \dots \\ \dots & \dots & \dots & \dots \end{bmatrix} \begin{pmatrix} a_1 \\ a_2 \\ a_3 \\ \vdots \end{pmatrix}. \quad (2)$$

Five terms ($N = 8$) are now chosen. Table 2 presents the coefficients a_i and the error between the chosen times with the burn-up values of 50 MWd/kgU. The sum of the coefficients a_i equals one. Essential cooling time period (important thermal-mechanical values in the rock are encountered) ranges from 20 to 2 000 years. The greatest interpolation error of the fit function in Table 2 is -0.385% (after 140 years).

The decay power 1 830 W (863 W/tU) of a canister is achieved with the burn-up value 50 MWd/kgU by cooling the fuel before deposition 49.9 years.

Table 2. Exponential presentation of EPR fuel decay heat. Burn-up value is 50 MWd/kgU.

i	Time [y]	Power [W/tU]	a_i	Error %
1	20 = t_1	1455.0 = P_1	0.09446	-
	30	1204.0		0.116
2	40	1013.0	0.20250	-
	50	862.9		-0.025
3	60	743.9	0.78708	-
	70	648.8		0.050
	80	572.5		0.068
	90	510.9		0.046
4	100	460.8	-0.50104	-
	110	419.9		-0.086
	120	386.3		-0.201
	140	335.1		-0.385
	160	298.5		-0.369
5	180	271.7	-0.257	-
	200	251.2		0.32343
6	1 000	77.64	0.06416	-
7	10 000	17.96	0.02662	-
8	100 000	1.498	0.00279	-

3 CALCULATION METHOD

Deformations and stresses are solved by finite element method. The applied finite element computer codes are described in (Ikonen 2001). Special properties like computation of temperatures are programmed inside the finite element codes. Temperatures are solved in a subroutine by analytic method, which has been shown to be very efficient in case of great amount of fuel canisters with varying decay heats (Ikonen 2005). Thermally induced stresses are summed to initially existing in-situ stresses in the rock material (described more in detail in Chapter 3.5).

3.1 Analytical solution of rock temperatures

The starting point of the analytic solution is a case, where heat energy of amount Q (unit e.g. J) in a point of infinite material (now rock) is released instantaneously. The temperature $T(r, t)$ at a certain time t and at a certain distance r from the heat source can be calculated from

$$T(r, t) = \frac{Q}{\rho c (4\pi d t)^{3/2}} e^{-\frac{r^2}{4 d t}}, \quad (3)$$

where $d = \lambda/(\rho c)$ is thermal diffusivity of the material (λ , ρ and c are thermal conductivity, density and thermal capacity of the material, respectively). In a xyz co-ordinate system the solution for a line heat source aligned vertically with z axis is obtained by integrating Equation (3) yielding (Hautojärvi 1987)

$$T(x, y, z, t) = \frac{QH}{\rho c 4\pi d t} e^{-\frac{x^2+y^2}{4 d t}} \frac{1}{2} \left\{ \operatorname{erf} \left[\frac{1}{2\sqrt{dt}} \left(\frac{H}{2} + z \right) \right] + \operatorname{erf} \left[\frac{1}{2\sqrt{dt}} \left(\frac{H}{2} - z \right) \right] \right\}, \quad (4)$$

where H is the height of the vertical line heat source. When the energy is released during longer time and the power P depends on time as in actual canister cases, Equation (4) is integrated with respect to time giving an analytical solution

$$T(x, y, z, t) = \frac{1/H}{\rho c 4\pi d} \int_0^t \frac{P(t')}{t-t'} e^{-\frac{x^2+y^2}{4 d (t-t')}} \cdot \frac{1}{2} \left\{ \operatorname{erf} \left[\frac{1}{2\sqrt{d(t-t')}} \left(\frac{H}{2} + z \right) \right] + \operatorname{erf} \left[\frac{1}{2\sqrt{d(t-t')}} \left(\frac{H}{2} - z \right) \right] \right\} dt', \quad (5)$$

where t' is the integration variable. In practice Equation (5) is integrated numerically. The assumptions concerning Equation (5) are that the material is homogeneous, it extends to infinity, has constant thermal diffusivity and the line heat source has uniform power generation. Superposing the solution of a number of single line heat sources the

temperature field of the whole repository can be determined efficiently. No effects from the groundwater flows are taken into account in thermal analyses.

The effect of non-zero canister radius r_0 can be corrected quite accurately substituting the actual height H of the canister by the effective height H_{eff} in the line heat source model (5)

$$H_{eff} = H + r_0 . \quad (6)$$

By using this height accurate results, as demonstrated in (Ikonen 2005), are obtained for the rock wall temperature from the analytical Equation (5). Then Equation (5) can thus be applied from the rock surface of the drilled hole. The decay heat power of a canister is 1830 W at deposition. The decay heat power at a certain time is different in each canister. The spacing between canisters along the tunnel is assumed to be 10 m. The spacing between tunnels is assumed to be 25 m.

3.2 Modelling of rock mechanics conditions

According to (Posiva 2005) the main rock type at Olkiluoto is migmatitic gneiss, which is highly heterogeneous. The types and amounts of foliation vary considerably. This rock is brittle and tends to lose its bearing capacity rapidly with even small levels of deformation. The critical strength and elastic properties of the other rocks types do not differ significantly from the migmatitic gneiss.

The mechanics properties of neither single fractures nor fracture zones have been measured directly in the laboratory or in the field. These properties can be estimated empirically based on geological description or rock mass classification techniques. The properties of the rock mass (intact rock matrix and fractures excluding fracture zones) have also been evaluated using rock engineering classifications, such as the Q-method. Q-values were found to be somewhat lower (indicating poorer rock quality) in the upper part of the bedrock (0 to 150 metres) than at greater depths (> 150 metres), where they are largely independent of depth. This conclusion is also supported by seismic velocity measurements, which showed Q-values for the rock mass about three to four times greater, indicating better rock quality than those associated to fracture zones. The average values of deformation modulus for the rock mass taken from velocity measurements are used in this thermal-mechanical analysis. Deformation modulus is about 50 GPa in higher depth and it is taken very conservatively to 25 GPa in the upper part (more fractured zones) of the bedrock (See Table 5.11 in Posiva 2005).

The pre-existing in-situ rock stress at Olkiluoto is affected by the mid-Atlantic Ridge push and by the postglacial rebound. In Fennoscandia, the major principal stress tends to be horizontal and is oriented NW-SE. The mid-Atlantic ridge push horizontal stress is estimated to be approximately 25 MPa. However, local variations in both magnitude and orientation are possible due to geological conditions, notably the major lineaments and brittle deformation zones. In-situ stress measurements in vertical boreholes were performed at depth ranging from 300 metres to 800 metres using either overcoring or hydraulic fracturing techniques, as shown in Figure 6.

Based on measurements (Figure 6) following regression lines for the stress components are presented

$$\begin{aligned}\sigma_H &= 0.047 z, 300 > z > 800 \text{ m} \\ \sigma_h &= 0.027 z, 300 > z > 800 \text{ m} \\ \sigma_v &= 0.024 z, 300 > z > 800 \text{ m},\end{aligned}\tag{7}$$

where σ_H and σ_h are the maximum and minimum horizontal stresses in MPa and z is the vertical depth from the ground surface [m]. Even if the fittings are said to be valid only in the interval from 300 m to 800 m, the measured point values indicate that the same fitting can be a good estimate for the interval starting from 0 m, ground surface (Olkiluoto Site Description 2004). Components according to Formula (7) are applied in three-dimensional analysis from 0 m to necessary depths in absence of better information.

3.3 Principal stresses

For evaluation of tensile stressed areas in the bedrock major principal stresses are determined. Principal stress components in three-dimensional case are solved from equation (Ylinen 1965)

$$\begin{aligned}\sigma^3 - (\sigma_x + \sigma_y + \sigma_z) \sigma^2 + (\sigma_y \sigma_z + \sigma_z \sigma_x + \sigma_x \sigma_y - \tau_{yz}^2 - \tau_{zx}^2 - \tau_{xy}^2) \sigma \\ - \sigma_x \sigma_y \sigma_z - 2 \tau_{yz} \tau_{zx} \tau_{xy} + \sigma_x \tau_{yz}^2 + \sigma_y \tau_{zx}^2 + \sigma_z \tau_{xy}^2 = 0,\end{aligned}\tag{8}$$

where the normal stress components are σ_x , σ_y , σ_z and the shear stress components are τ_{xy} , τ_{yz} , τ_{zx} . The major principal stress σ_{maj} is defined as the highest absolute value of the three roots of Equation (8).

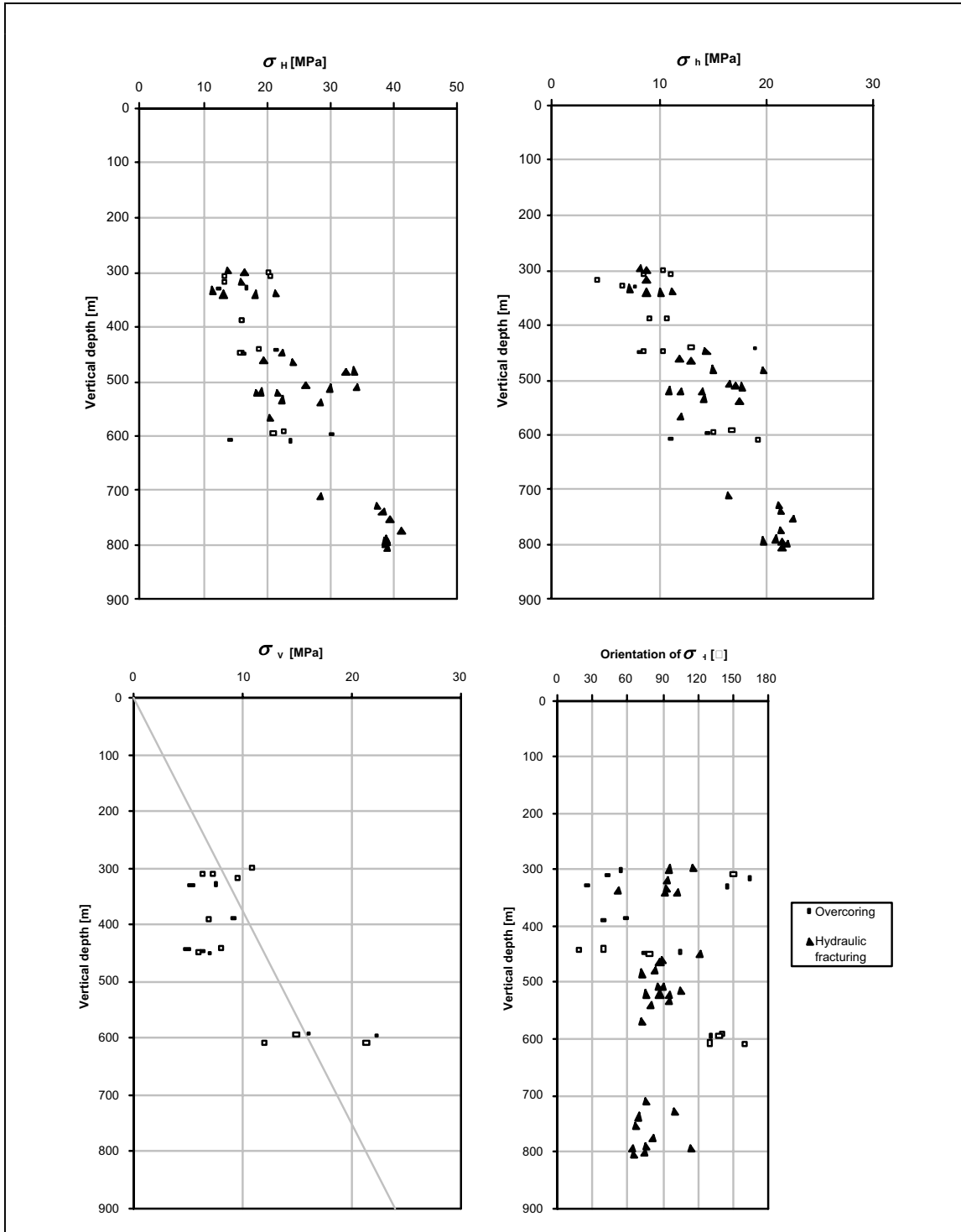


Figure 6. Magnitudes of the horizontal and vertical stress components, and orientation of the maximum horizontal stress, as inferred from overcoring and hydraulic fracturing measurements. (For the vertical stress, a theoretical line corresponding to the overburden stress is shown for reference). (Posiva 2005, page 133).

3.4 Modelling of fractured rock on tensile stressed volumes

The fractured rock mass may be modelled by different ways. Mohr-Coulomb (Drucker-Prager) material model or modelling of non-tension material as described for instance in (Zienkiewics 1977) are generally applied. One possibility is the modelling of actual fractured zones with their orientation as done in (Hakami 1998). Because of several uncertainties and lack of detailed information, however, a simple engineering approach is here adopted. It is assumed that the rock material behaves in isotropic way despite of fracture and only modulus of elasticity is reduced, if the major principal stress is in tension.

3.5 Analyzing procedure

For evaluation the effect of tension fractured rock, first analyses with intact rock mass modelling are performed. In such analyses the procedure is straightforward. At a chosen time the temperatures are determined from analytic formulae like presented in Chapter 3.1 and linear-elastic analyses are performed assuming no initial stresses. After solution the stress components the initial stress components are summed to these solved components and principal stresses are determined. Repeating linear-elastic analyses stepwise in time, the evolution of some quantity, like the uplift of the ground surface, is obtained.

In case of tension fractured rock mass model the solution is time dependent and an analysis is advanced by taking sufficiently short time increments (e.g. 10 years). Initial stresses are taken into account only in solving the first time step by summing the solved and initial stress components. The summed stress components in all the integration points are stored for following time steps and they are updated in advancing the calculation. Temperature differences solved from analytic formulae during every time step cause thermal loading. If the major principal stress changes during a time step from compression to tension in some of integration (Gaussian) point of the elements, modulus of elasticity and the stiffness matrix of the whole model is updated. Analyses with tension fractured rock mass modelling mean isotropic softening of rock material. Other possible material behaviour like time dependent creep on highly stressed volumes is not considered.

4 TWO-DIMENSIONAL ANALYSES

Temperature and stress fields of actual repositories are three-dimensional. For making faster pre-analyses and many parametric studies first, a large number of two-dimensional analyses are performed. The dimension of the model was determined by 2D analyses. The width 4 000 m and the height 2 000 m of the model were determined by trial-and-error method so far from the repository that the disturbances from the repository area do not reach the right and left vertical and horizontal lower planes. Also the sufficient short time increment of 10 years in case of tension fractured rock mass modelling was determined by 2D analyses. Two-dimensional analyses are further important for setting-up the model for three-dimensional analyses. Analyses with homogeneous rock modelling at different times are performed by repeating linear-elastic analyses.

Initial stresses are evaluated from Equations (7). As a result of a plane strain analysis three normal stress components are obtained, two of them in plane (xy -plane, x horizontal and y vertical) and the third out of plane (z horizontal). The horizontal tensile stress induced by thermal load reaches higher value in the x -direction than in z -direction, since in this out-of plane direction temperature remains constant to infinite in the plane strain model. For this reason 2D analysis gives incorrect ratio of different horizontal stress components, even if the magnitude is correct. That is why orientation of the in-situ stresses are not considered here but in connection of 3D analyses in Chapter 5. The lower horizontal initial stress component σ_h is summed to σ_x and vertical σ_v is summed to σ_y .

In xy -plane the major principal stress is computed from

$$\sigma_{maj} = \frac{\sigma_x + \sigma_y}{2} + \frac{1}{2} \sqrt{(\sigma_x - \sigma_y)^2 + 4\tau_{xy}^2} . \quad (9)$$

In this formula the stress components are summed components. The stress computed from Equation (9) is compared to transverse stress and the greater one is chosen as the major principal stress.

4.1 One-storey repository with intact rock mass model

Analyses with intact rock mass modelling at different times are performed by repeating linear-elastic analyses. Figure 7 shows the element mesh of the plane strain model of the repository and surrounding rock. Eight-noded isoparametric elements are applied. There are 206 elements and of 649 nodes. The material properties used in the analysis are according to the specification in Chapter 2. In forming the stiffness matrix of an element the integration order is 3x3 in order to capture more points than using order 2x2. The size of the stiffness matrix of the whole model is 124 723.

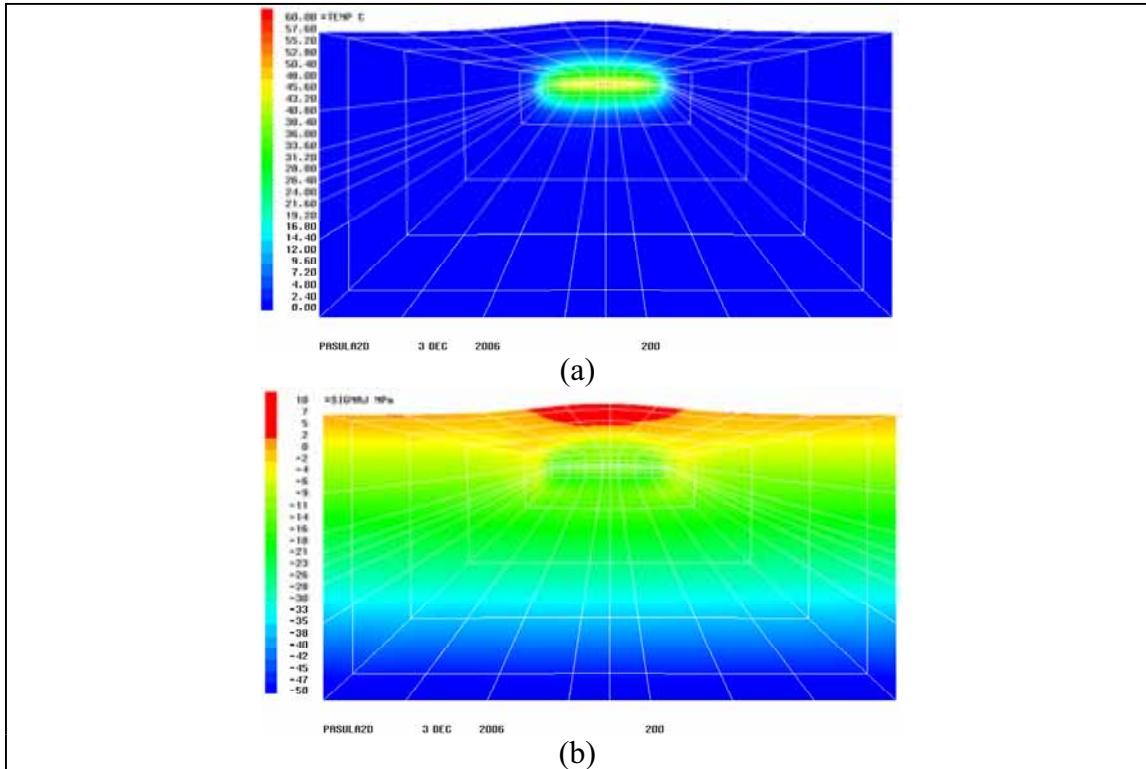


Figure 7. Temperatures (a) and major principal stresses (b) after 200 years, when deepest tensile stressed area (red colour) is encountered (deformations multiplied by 1000).

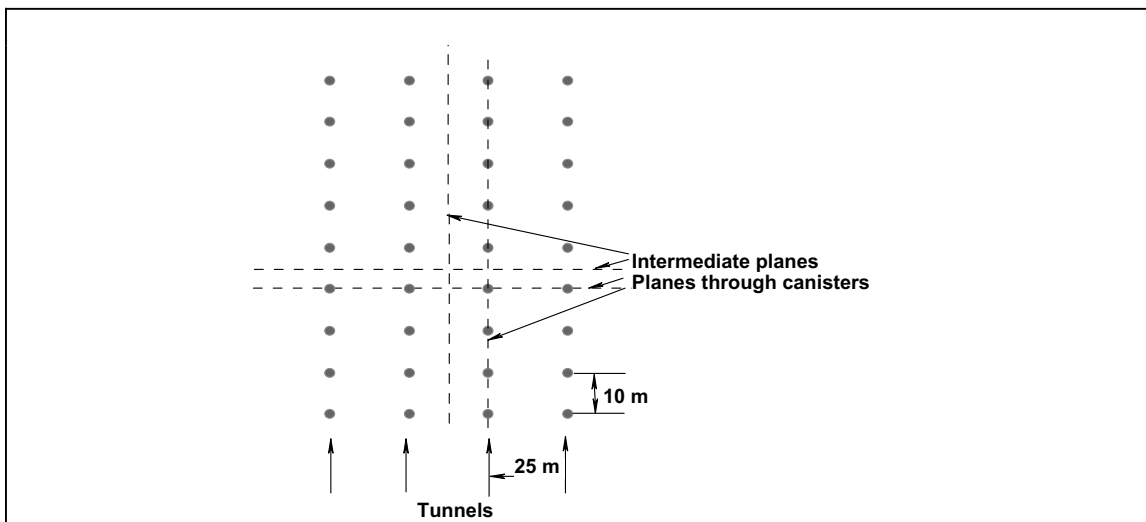


Figure 8. Location of the 2D model cross-section plane is varied.

In the model the horizontal displacements are constrained on the left and right vertical end planes and the lower horizontal plane vertical displacements are constrained. In the two-dimensional model plane strain condition is assumed. This means that strains on

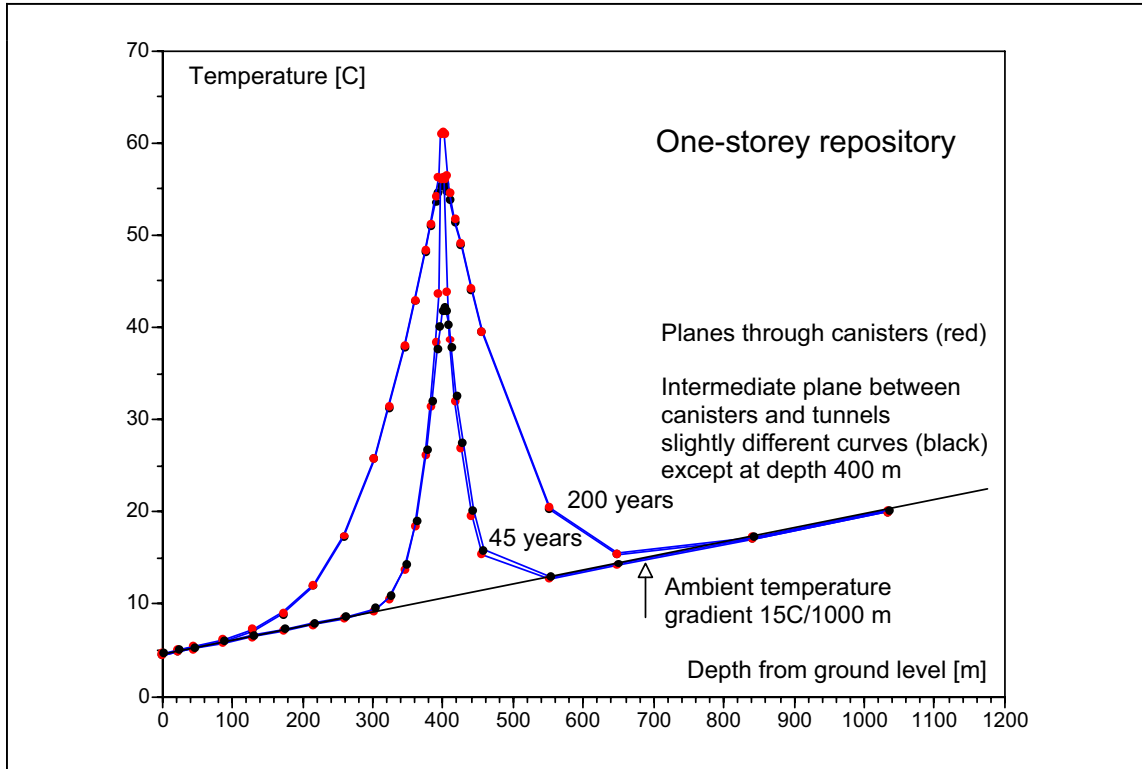


Figure 9. Vertical temperature distribution along vertical middle line in the rock after 45 years, when all canisters are deposited and after 200 years, when the deepest tensile stressed area is encountered (see also Figure 10).

perpendicular direction of the plane are constrained. Figure 7a shows temperature distribution and Figure 7b major principal stress distribution after 200 years, when the deepest tensile stressed area is encountered.

The increase of the ambient temperature in depth direction in the rock is $15^{\circ}\text{C}/1000\text{ m}$ (Figure 9). This temperature gradient is not taken into account in the analysis, since it is assumed that the ambient temperature distribution has no effect on the initial in-situ stresses. They are constant in time and shape outside the repository disturbed area.

Figure 9 shows temperature distributions after 45 and 200 years either in a case that the cross-section passes through the canisters or in a case, where the cross-section locates in the intermediate plane. In the former case the temperatures are overestimated and in the latter case they are underestimated. In both cases the temperature distributions are very close to each other's except at very near the canisters. This area is so narrow that the differences have insignificant effect on far-field values near the ground surface. The curve showing the tensile stressed depth in Figure 10 was first calculated by setting the plane through canisters (preference/default case). The case, where the plane passes through the intermediate plane gave almost identical curve. Also the case, where all the canisters were deposited simultaneously, gave almost identical curve after 150 years. The effect of the element mesh density was studied by doubling the mesh (Figure 11) in the default case. Only small difference can be observed in the tensile stressed depth curve (plotted without symbols). The width of the tensile stressed area on the ground

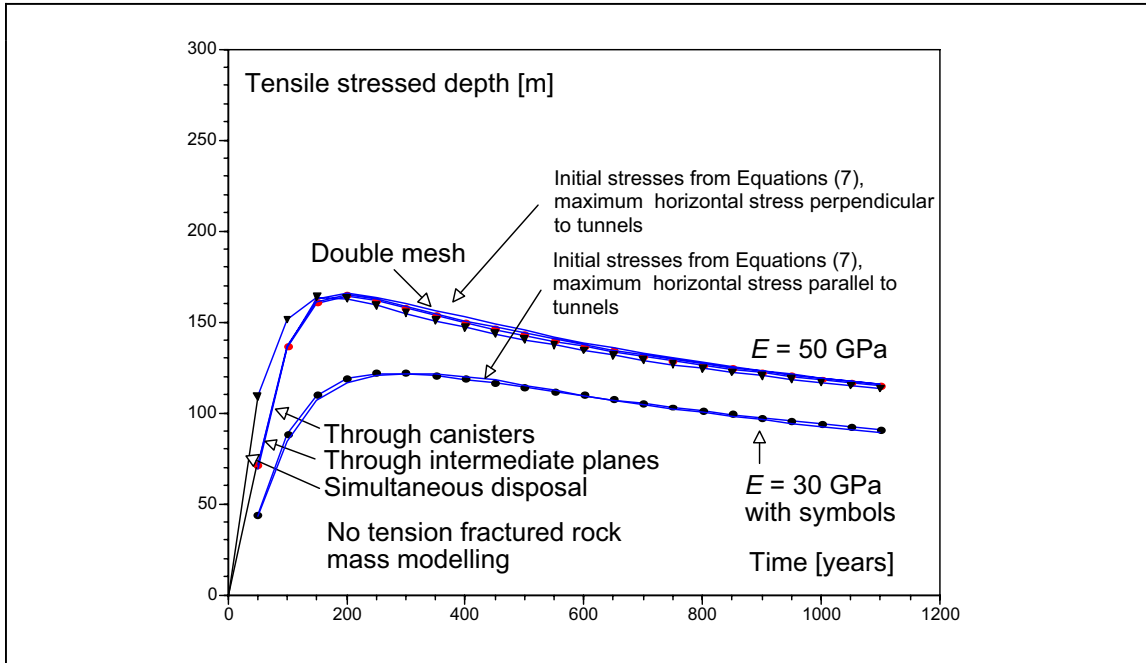


Figure 10. Tensile stressed depth in rock in middle of model.

surface is nearly constant and about 1100 m for long times. Also the two-storey case was studied and similar results were obtained. Due to higher thermal load tensile stressed depth increased about 50 m.

The depth of tensioned rock volume reaches its maximum 163 m at about 200 years after deposition (Figure 10). An important input parameter for the analysis is the deformation modulus of the rock mass. Figure 10 demonstrates that lowering of deformation modulus from 50 GPa to 30 GPa, the maximum depth is decreased significantly.

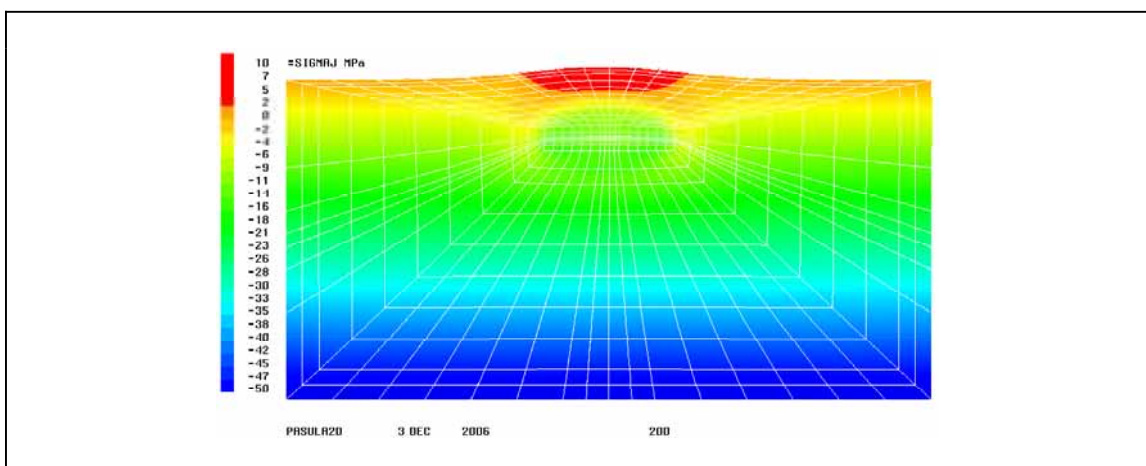


Figure 11. Stresses with double density mesh after 200 years, when deepest tensile stressed area (red colour) is encountered (deformations multiplied by 1000).

4.2 Two-storey repository with tension fractured rock mass model

Special routines were developed for automatic mesh generation. Figure 12 shows major principal stress distribution after 200 years, when deepest tensile stressed area is encountered. Similar stress distribution pattern is obtained as in case without tension fractured rock mass modelling (Figure 7b). The maximum depth 230 m is 15 m greater than with intact rock mass model.

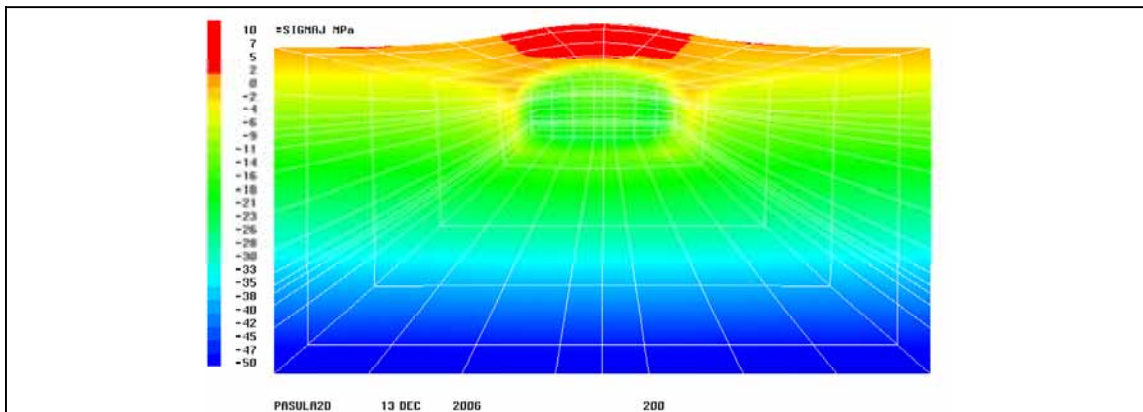


Figure 12. Major principal stresses and deformations in the bedrock after 200 years, when deepest tensile stressed area (red colour) is encountered (deformations multiplied by 1000). Deformation modulus reduced by 2 on tensile stressed areas (red colour in figure).

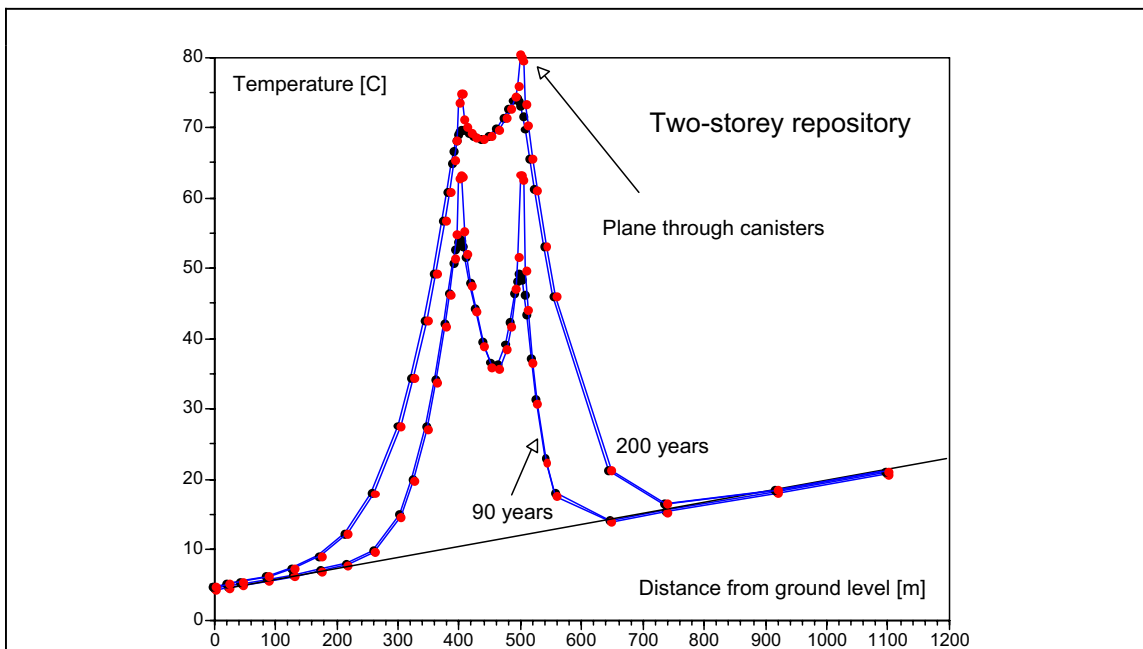


Figure 13. Vertical temperature distribution in the rock after 90 years, when all canisters are deposited and after 200 years, when deepest tensile stressed area is encountered (see Figure 14).

Figure 13 shows temperature distributions after 90 and 200 years either in a case that the cross-section passes through the canisters or in a case, where the cross-section locates in the intermediate plane, see Figure 8. They give very similar far-field results. Rather high temperature (greater than 80 °C in Figure 13) is reached in the lower repository at 200 years after deposition. This great value is caused by the fact that the decay power of the lower repository was conservatively assumed to be identical and as high as in one-storey repository.

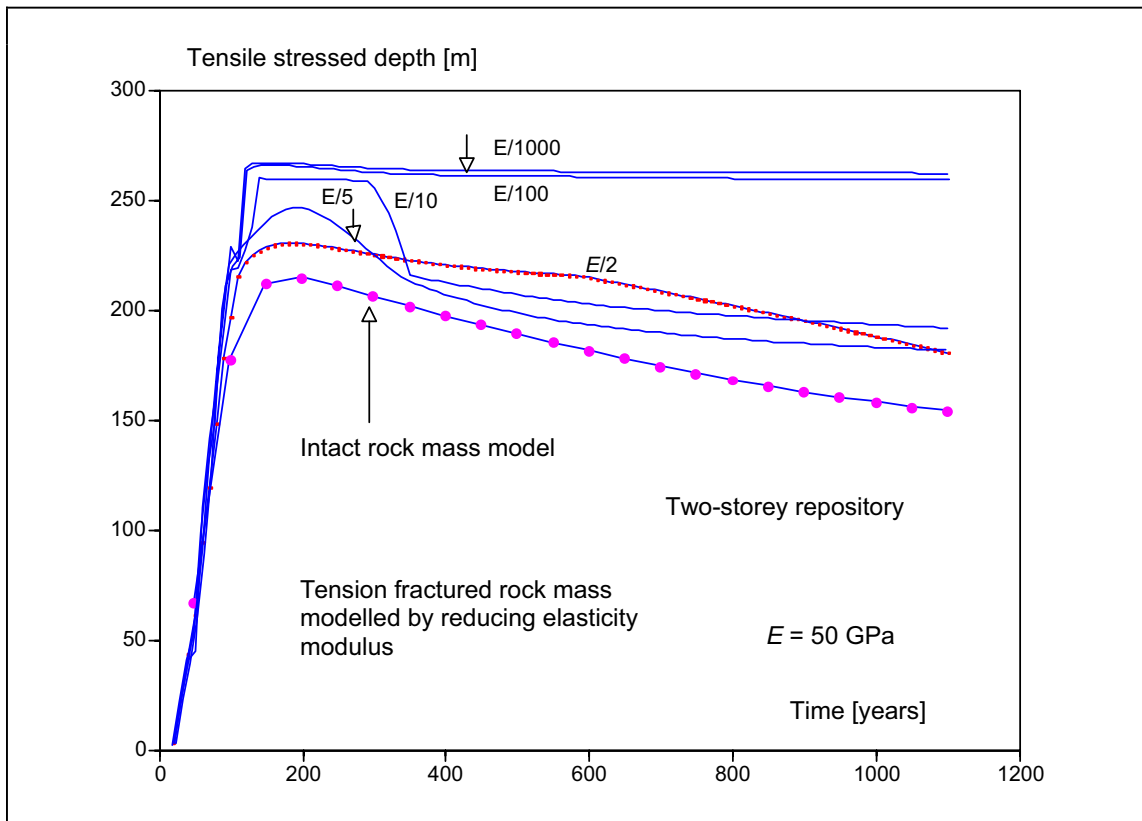


Figure 14. Tensile stressed depth in the rock.

Figure 14 shows also the effect of further reducing the deformation modulus. The maximum tensile stressed depth seems to saturate to the depth of 266 m. This can be explained by the fact that compressive in-situ stresses are high enough to hinder the stress state to become tensile.

The effect of the element mesh density was studied by doubling the mesh density. Similar principal stress patterns were achieved and nearly equal results were obtained and evidently the coarse mesh in Figure 12 is gives sufficiently accurate results.

4.3 Effect of depositing rate

In the following all the canisters are deposited simultaneously. Figure 15 demonstrates that the shape of the curve is nearly identical with the curve of the non-simultaneous deposition, but there is a shift of about $90/2 = 45$ years (in one-storey repository about $45/2 = 22.5$ years). The maximum depths are nearly equal. The result is natural because of considering far-field quantity after long times. The simultaneous deposition gives slightly conservative value for the maximum depth. It can be concluded that simultaneous deposition gives practically equal maximum tensile stressed depth as the actual deposition rate of some 20 canisters per year. This result is applied in later three-dimensional analyses in order to reduce the size of the finite element model.

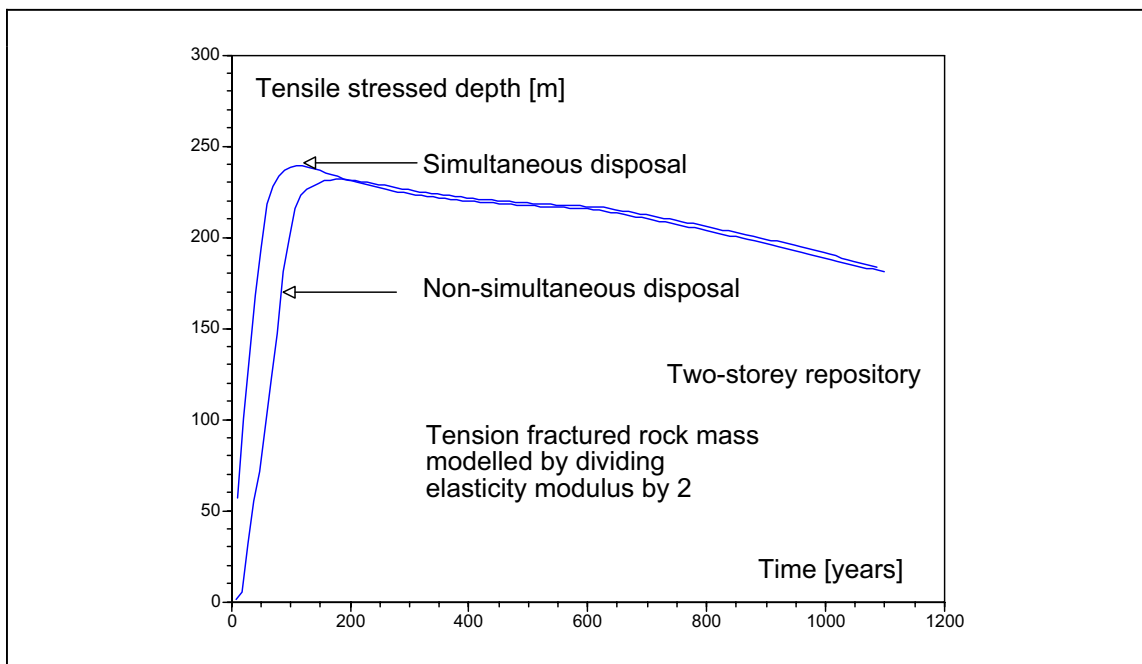


Figure 15. Tensile stressed depth in the bedrock. Comparison of simultaneous and non-simultaneous deposition.

4.4 Conclusion from 2D analysis

The analyses above show that simultaneous deposition gives practically equal maximum tensile stressed depth as the actual deposition rate of some 20 canisters per year.

The shape of tensile stressed volume is very similar in different cases and the width on the ground surface is very constant for long times. In case of two-storey repository the maximum tensile stressed depth is about 50 m deeper than in case of one-storey repository. Effect thermal conductivity was studied by increasing the conductivity by 10% and the maximum of the tensile stressed depth 230.86 m in Figure 15 in case of non-simultaneous deposition decreased only by 1.2 % to 230.07 m.

5 THREE-DIMENSIONAL ANALYSES

As in Chapter 4.3 it was concluded, simultaneous deposition gives practically equal maximum tensile stressed depth as the actual deposition rate. In case of simultaneous deposition there are thus two vertical planes of symmetry and the size of the three-dimensional model can be remarkably reduced. A quarter is sufficient to be modelled. A cube around the repository centre is much enough to be modelled. The edge of the cubic 3D model is 2 000 m corresponding the dimension in 2D analyses. The volume is divided into 20-noded isoparametric elements. The model plotted in Figure 16 has 412 elements and 2 190 nodes. The front face of Figure 16 is identical with the right half of the two-dimensional model (see e.g. Figure 7). In transverse direction (the direction of the tunnels) there are 4 element layers. The number of degrees of freedom is 6 053 and the size of the stiffness matrix is 4 166 789. The nodes lying in the vertical end planes were constrained in horizontal direction and the nodes on the lower plane in the dept of 2 000 m were constrained in vertical direction. In forming the stiffness matrix of an element the integration order is 3x3x3. The number of degrees of freedom is 11 522 and the size of the stiffness matrix is 10 739 059.

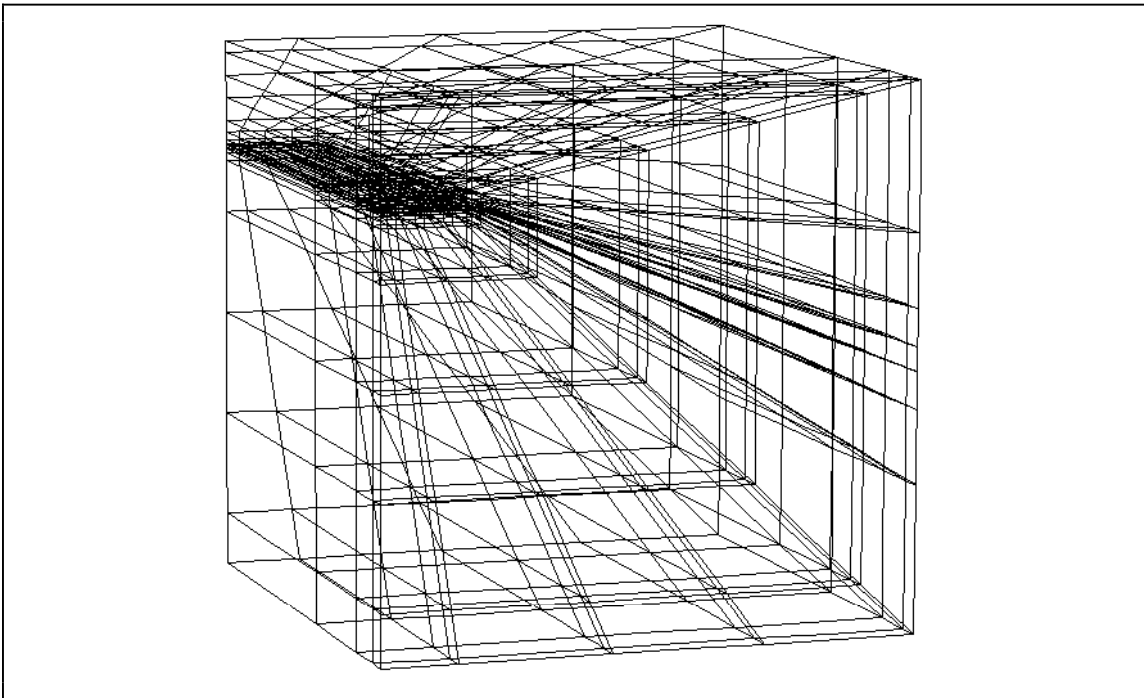


Figure 16. 3D finite element mesh.

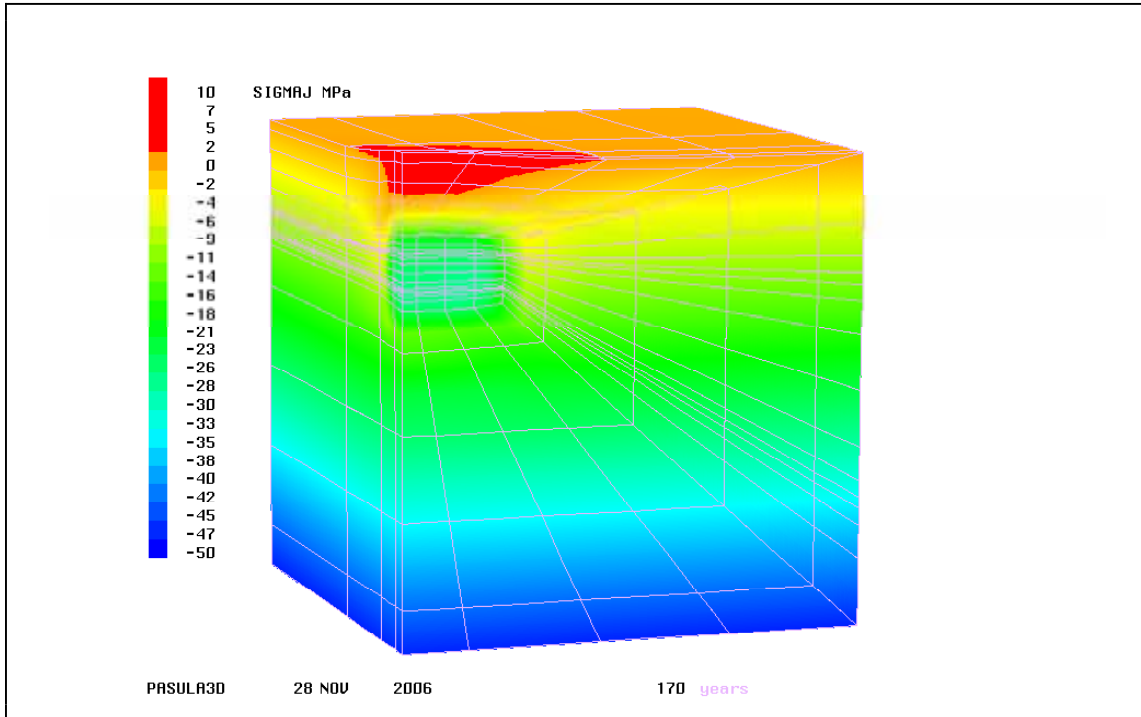


Figure 17. Stresses after 170 years, when the deepest tensile stressed area (red colour) is encountered (deformations multiplied by 1000).

Figure 18 shows the effect of the orientation of the tunnels with respect to horizontal initial stress components computed from Equations (7). The horizontal tensile stress induced by thermal load reaches higher value in the direction of the shorter dimension of the panel (in the tunnel direction) than in the longitudinal direction of the panel. In order to compensate this stress as much as possible the higher compressive in-situ stress σ_H should be applied to the direction of the shorter side of the panel to lower tensile stressed depth (the lower curve in Figure 18). The maximum depth of the tensile stressed volume is obtained, if the direction of the higher compressive in-situ stress σ_H is applied perpendicular to the tunnels. This kind of repository layout is very unlike, because the tunnels are generally oriented parallel to the maximum horizontal in-situ stress in order to lower the compressive stress around tunnels. If the actual orientation deviates from these extremes, a curve falls apparently between the two curves shown in Figure 18.

Because of simultaneous deposition of the canisters in three-dimensional analyses the times for maximum values are about 22.5 years earlier in the one-storey case and about 45 years earlier in the two-storey case than in actual dispositions.

In case that the maximum in-situ horizontal stress is oriented parallel to tunnels, the maximum tensile stressed depth 146 m is achieved after 380 years. In case that the in-situ stress is oriented perpendicular to tunnels, the maximum depth 195 m is achieved after 170 years. The difference in the maximum tensile stressed depths is 49 m.

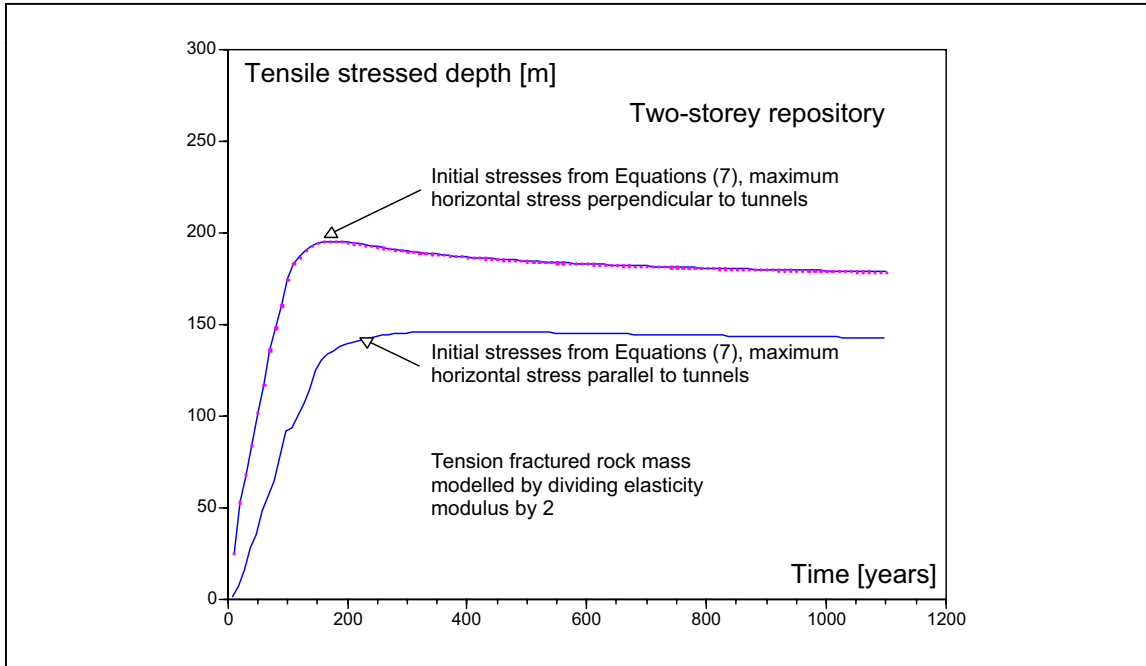


Figure 18. Tensile stressed depth in rock with various assumptions of initial stress distribution.

In the following results the tunnels are oriented parallel to the maximum horizontal in-situ stress.

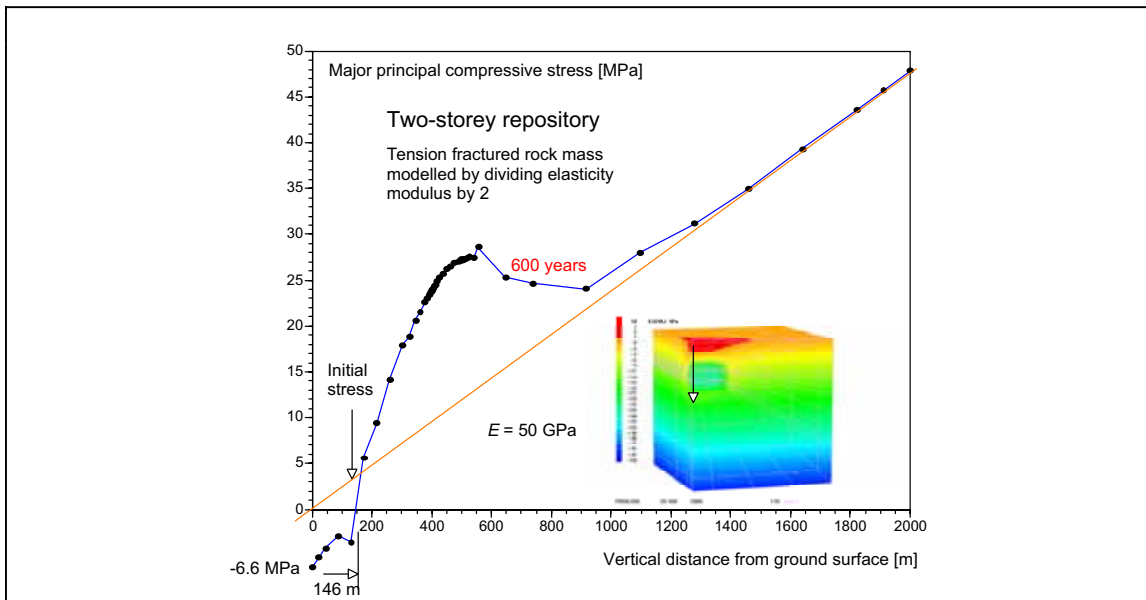


Figure 19. Major principal compressive stress history in the middle of the repository along the front vertical corner.

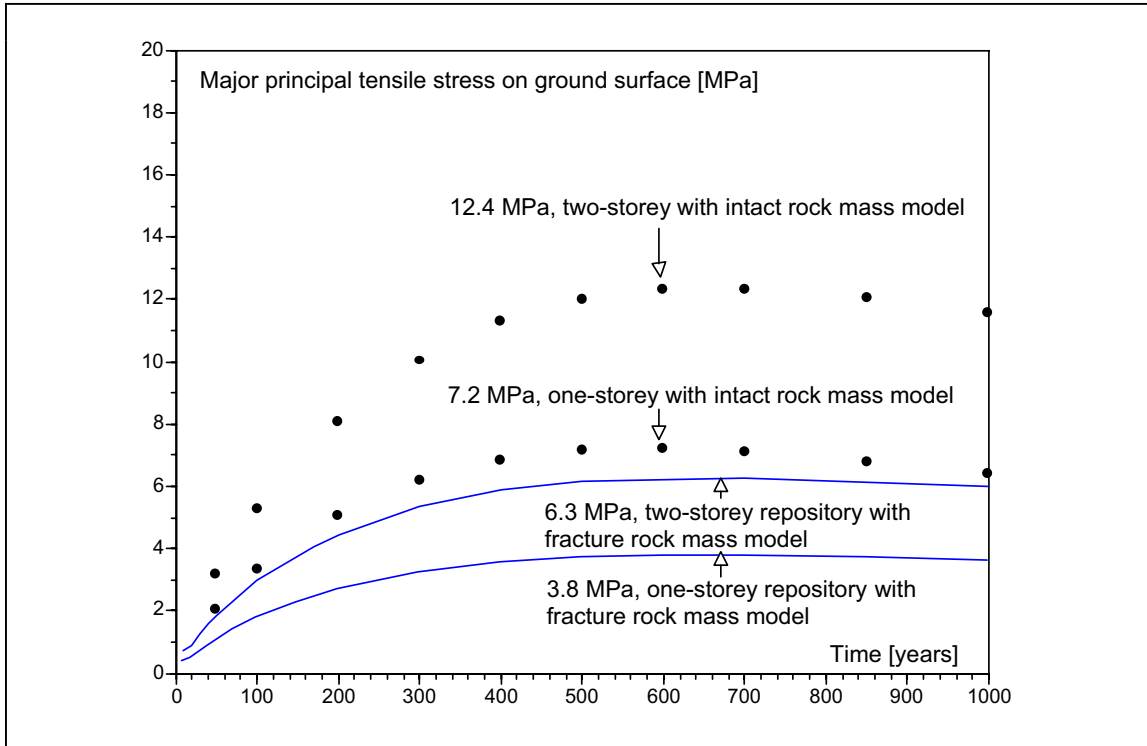


Figure 20. Major principal tensile stress evolution on ground surface.

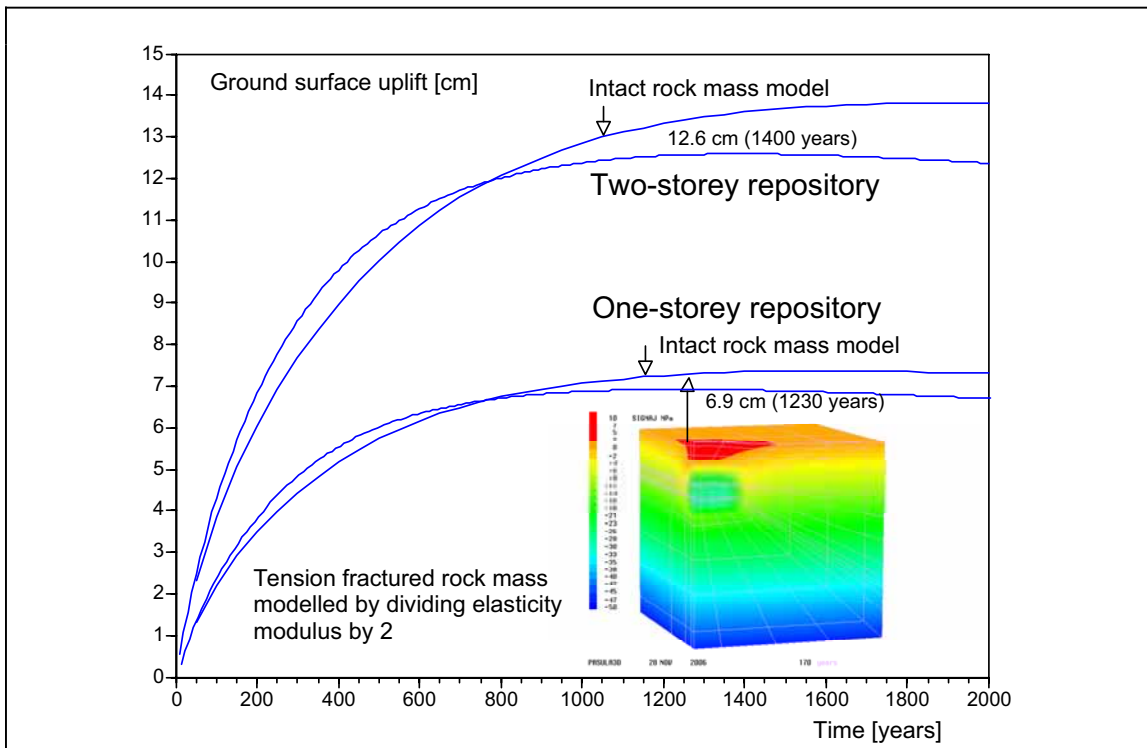


Figure 21. Ground surface uplift evolution in the middle of model.

Ground uplift reaches its maximum of 6.9 cm about 1 230 years in the one-storey repository and 12.6 cm in the two-storey repository after about 1 320 years.

Figures 22 and 23 show the strain evolution on the ground surface in the direction of the tunnels and in the transverse direction. Due to two vertical symmetry planes of the model these strains are the principal strains and the strain in the direction of the tunnels is the other principal strain. The maximum value of about 0.00024 is reached after 600 years.

The width and length of the tensile stressed area on the ground surface are about 600 m and 1000 m and they stay nearly constant for very long times (Figures 22 and 23). The corresponding dimensions of deposition block are 310 m and 725 m.

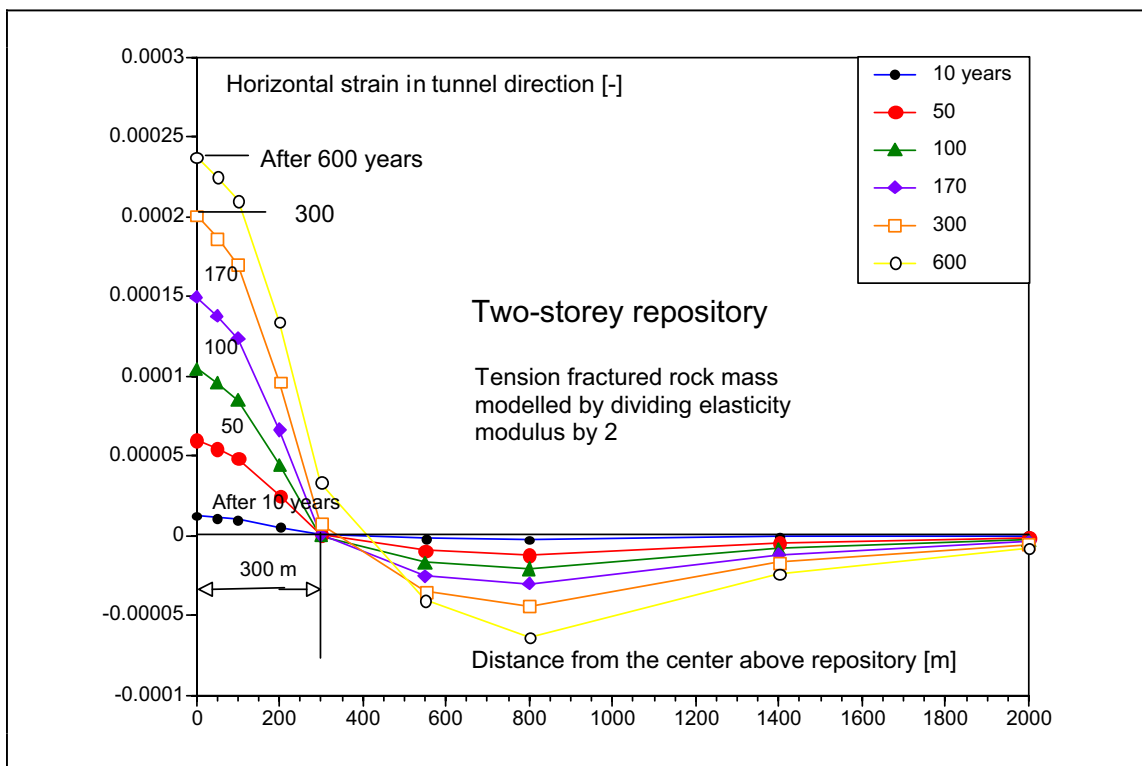


Figure 22. Horizontal strain distributions on ground surface in direction of tunnels.

Numerical solution took about 2 hours of CPU time in a HP workstation in case of the two-storey repository with tension fractured rock mass model.

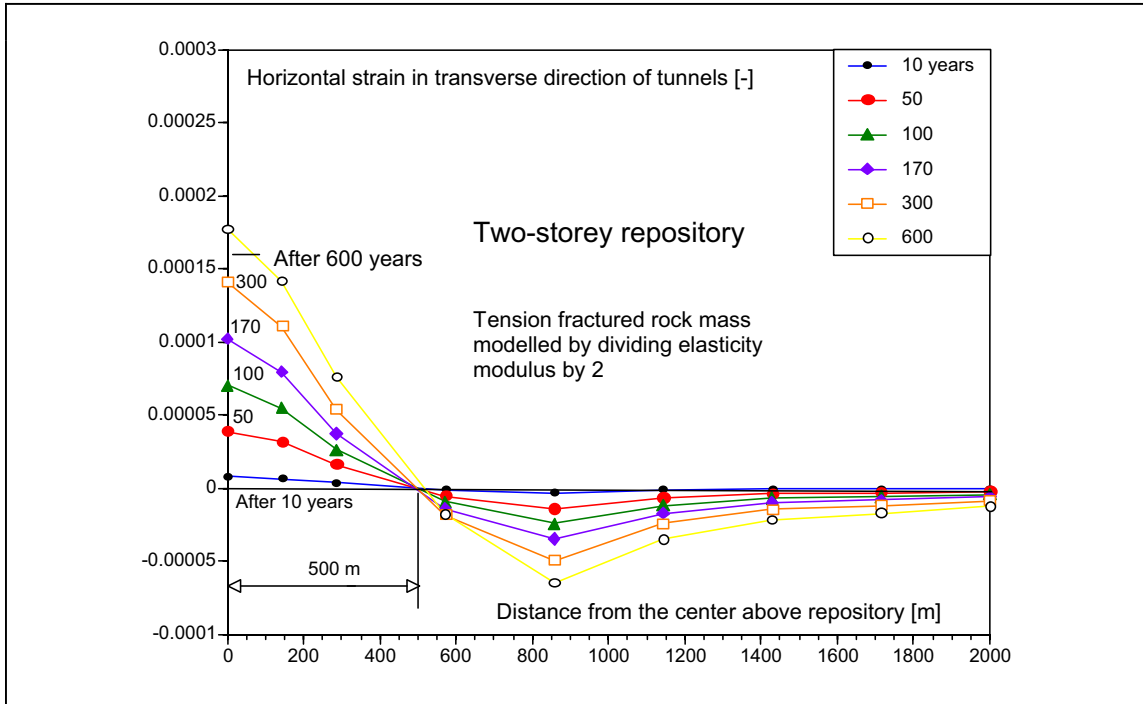


Figure 23. Horizontal strain distributions on ground surface in transverse direction of tunnels.

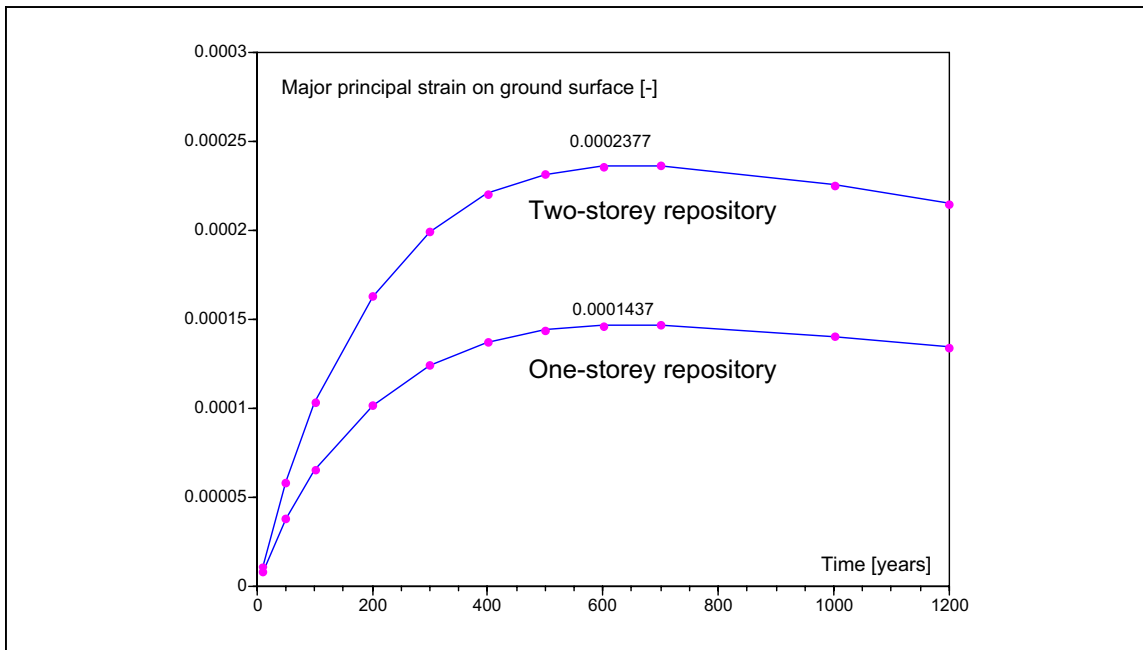


Figure 24. Major principal tensile strain evolution in tunnel direction on ground surface.

If there were vertical fractures above the centre of the repository on the ground surface evenly distributed at one meter intervals, and the stress state would be fully relaxed in the neighbourhood of the fractured rock area, all the cracks would open 0.24 mm, at maximum, after 600 years (Figure 25). Horizontal fractures are not relevant to be considered, since they are not opened due to stationary compressive vertical stress component.

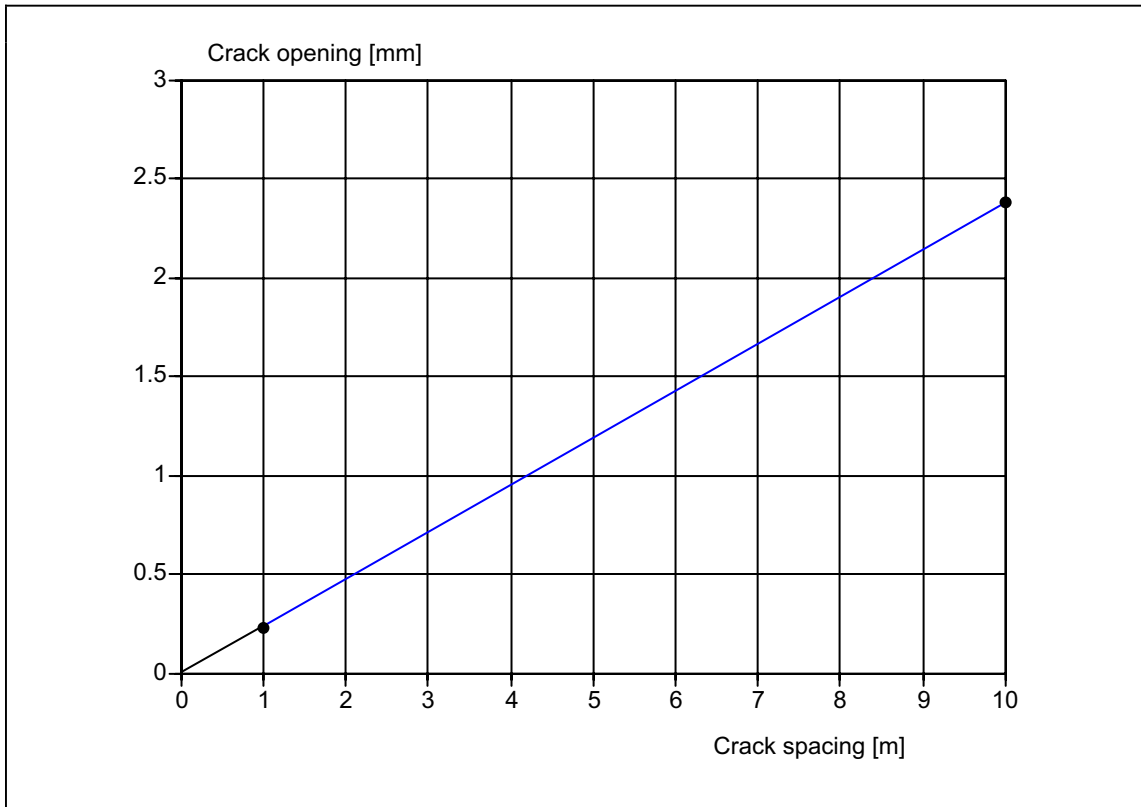


Figure 25. Estimate of an ideal crack opening as a function of crack spacing. The curve is obtained by multiplying the strain 0.00024 by the postulated crack spacing.

The volume of the tensile stressed rock is significant and the duration of that period is about 2 000 years.

5.1 Conclusion from 3D analysis

Two-storey repository causes about 50 m deeper tensile stressed bedrock volume than the one-storey repository.

Due to thermal expansion, the rock mass is lifted upwards, and the maximum uplift at the ground surfaces is calculated to be 7 cm in the one-level after about 1 250 years repository and 12 cm in the two-level repository after about 1 320 years. The amount of fractured rock effects only a little on these displacements.

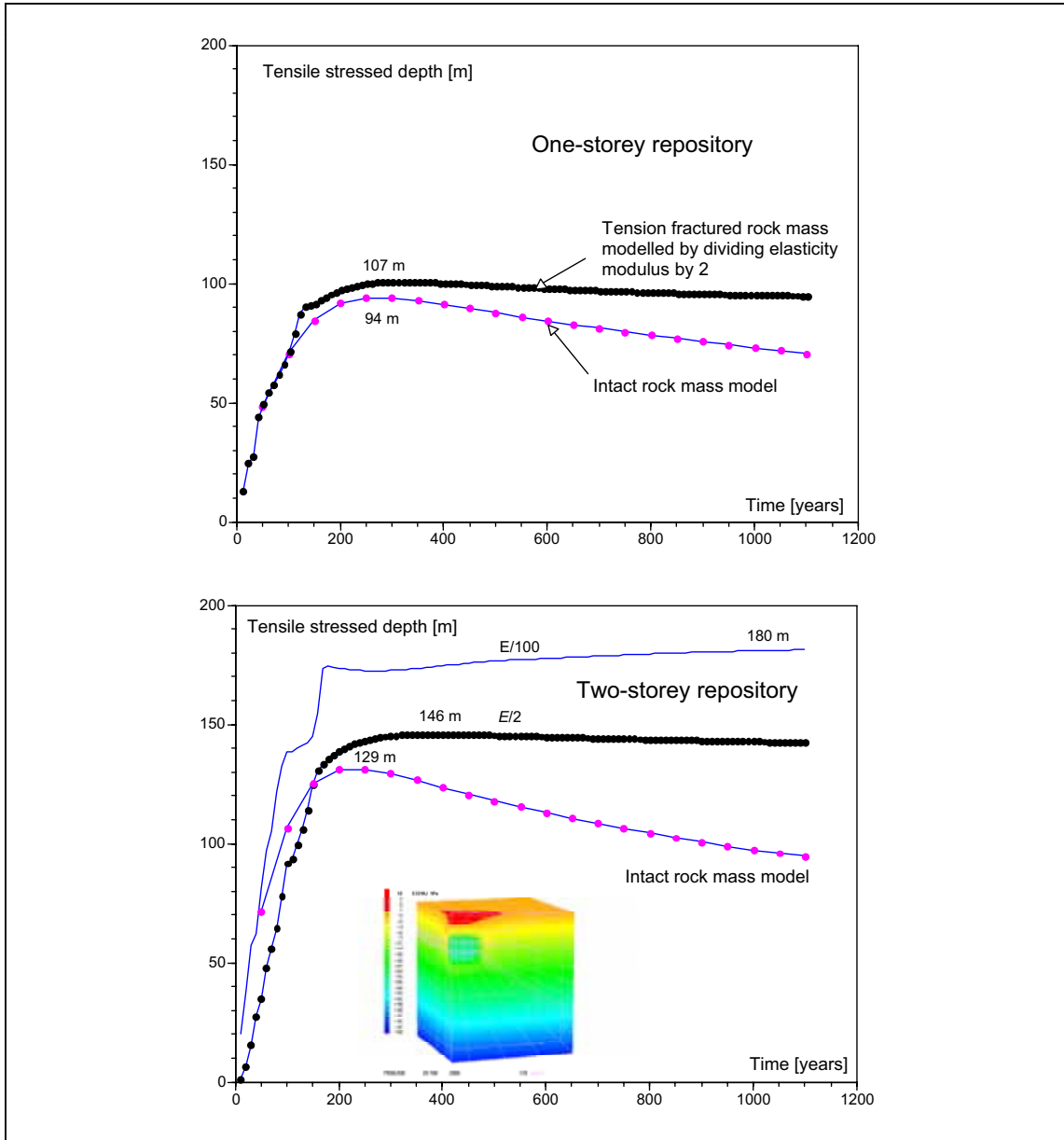


Figure 26. Tensile stressed depth in rock in different cases. Initial stresses determined according to Equations (7) and maximum horizontal in-situ stress is parallel to the tunnels.

Figure 26 shows that in case of one-storey repository the intact rock mass model gives the maximum tensile stressed depth 94 m and the model including fractured rock gives 107 m. In case of two-storey repository the corresponding depths are 129 m and 146 m. Figure 26 shows also the effect of further reducing the deformation modulus in tensile stressed volumes in case of two-storey repository. The maximum of the tensile stressed depth saturates to 180 m. This can be explained by the fact that in-situ stresses are high enough below 180 m to hinder the stress state to become tensile. The tensile stressed volume and its width decreases with increasing deformation modulus.

6 CONCLUDING REMARKS

The objective of this study was to investigate far-field thermal-mechanical behaviour of the rock above one- and two-storey repositories.

In the volume close to the ground surface, the initial horizontal compressive stresses are reduced due to increasing tensile stresses caused by thermal expansion on the repository level. Thus the major principal stress component is changed from compression to tension to the depth, which depends on the magnitude of the thermal power on the repository area. The depth is about 50 shallower in the one-storey repository than in the two-storey repository due to lower heat power in former case.

The depth in tensioned volume extends in the one-storey repository to 94...107 m after about 200 years and in the two-storey repository to about 129...146 m. Modelling of tension fractured rock in tension stressed rock volume by lowering the deformation modulus increases the maximum depth of the tensile stressed rock at most 10%.

The actual planned deposition rate and the postulated simultaneous deposition (all canisters are deposited at a time) give practically equal long-time far-field response.

Table 3 summarizes the main results from the analyses. In general, the results are in a fairly good agreement with the results presented in (Hakami 1998).

The numerical results based on very limited amount of available exact in-situ information of the existing natural stress conditions in Olkiluoto bedrock. For example, there was no measured in-situ stress information from 0-200 m depth.

The results are sensitive to the deformation modulus of the intact rock mass and the orientation of the panel in the in-situ stress field, if the rectangular panel deviates from a square shape. The tension stressed depth reaches its minimum, if the maximum horizontal in-situ stress is parallel to the shorter side of the panel. With the analyzed panel aspect ratio the effect is 50 m in the tension stressed depth.

Table 3. Main results from 3D analyses.

Intact rock mass modelling	Maximum depth of tensile stressed rock volume	Ground surface uplift	Major ground surface stress	Horizontal maximum surface strain
One-storey repository	94 m after 300 years	7.4 cm after 1600 years	7.2 [MPa] after 600 years	0.0000065 after 1100 years
Two-storey repository	129 m after 300 years	13.8 cm after 2000 years	12.4 [MPa] after 700 years	0.000014 after 1100 years
Tension fractured rock mass modelling				
One-storey repository	107 m after 320 years	6.9 cm after 1230 years	3.8 [MPa] after 700 years	0.00015 after 700 years
Two-storey repository	146 m after 380 years	12.6 cm after 1400 years	6.6 [MPa] after 600 years	0.00024 after 600 years

ACKNOWLEDGEMENT

Professor John A. Hudson, Dr. Jonny Sjöberg and Mr. Erik Johansson are highly appreciated for their informative and professional comments on the draft report.

Mr. Heikki Raiko of VTT is gratefully acknowledged for planning the guidelines of the work, useful discussions and reviewing the report.

REFERENCES

- Anttila, M. 2005. Radioactive Characteristics of the Spent Fuel of the Finnish Nuclear Power Plants. Working Report 2005-71. Posiva Oy, Olkiluoto. 20 p + App. 310.
- Hakami, E., Olofson O., H., Israelsson, J. 1998. Global thermo-mechanical effects from a KBS-3 type repository. Summary report. Technical report 98-01. Svensk Kärnbränslehantering Ab (SKB), Stockholm. 39 p.
- Hautojärvi, A., Anttila, M. & Taivassalo, V. 1987. Effects on fuel burn-up and cooling periods on thermal responses in a repository for spent nuclear fuel. Report YJT-87-21. Technical Research Centre of Finland. 32 p.
- Ikonen K. 2005, Thermal analysis of repository for spent EPR-type fuel. Report POSIVA 2005-12. Posiva Oy, Olkiluoto. 36 p. ISBN 951-652-138-X.
- Ikonen K. 2003. Thermal analysis of spent nuclear fuel repository. Report POSIVA 2003-4. Posiva Oy, Olkiluoto. 61 p. ISBN 951-652-118-5.
- Ikonen K., 2001. Large inelastic deformation analysis of steel pressure vessels at high temperature. Technical Research Centre of Finland. Doctoral thesis. VTT Publications 437. ISBN 951-38-5856-1. 141 p + App. 15 p.
- Jussila, P. 1997. Analytical solutions of the mechanical behaviour of rock with applications to a repository for spent nuclear fuel. Report STUK TR 136, Helsinki. 38 p + App. 17. ISBN 951-712-230-6.
- Kukkonen, I. 2000. Thermal properties of the Olkiluoto mica gneiss: Results of laboratory measurements. Posiva Oy. Working Report 2000-40. 28 p.
- Posiva , 2005. Olkiluoto Site Description 2004. Report POSIVA 2005-03. Posiva Oy. 444 p. ISBN 951-652-135-5.
- Paulamäki, S., Paananen, M., Kärki, A., Gehör, S., Front, K., Aaltonen, I., Ahokas, T., Kemppainen, K., Mattila, J., Wikström, L. 2006. Geological model of the Olkiluoto site v. 0. Posiva Oy, Olkiluoto, Finland. Posiva Working Report 2006-37.
- Raiko, H. 2005. Disposal canister for spent nuclear fuel – design report. Report POSIVA 2005-02. Posiva Oy, Olkiluoto. 61 p.
- Ylinen, A. 1965. Kimmo- ja lujuusoppi. Werner Söderström Osakeyhtiö. Porvoo. 1010 p.
- Zienkiewicz, O.C. 1977. The finite element method. 3. edition. McGraw-Hill. London. 787 p.